REGISTERED NO. M. 3121

UNIVERSITY OF MICHIGAN
AUG 23 1957
PHYSICS LIBRARY

PROCEEDINGS
OF THE
INDIAN ACADEMY
OF SCIENCES

VOL. XLV] *SECTION A* [No. 6

JUNE 1957

Price Rs. 2 or 3 Sh. *Annual Subscription Rs. 18*

PRINTED AT THE BANGALORE PRESS, BANGALORE CITY, BY C. VASUDEVA RAO
SUPERINTENDENT AND PUBLISHED BY THE INDIAN ACADEMY OF
SCIENCES, BENGALORE.

STUDIES ON COLLAGEN

II. Cylindrical Lattice Structure of Collagen

By V. Sasisekharan and G. N. Ramachandran, F.A.Sc.

(*Department of Physics, University of Madras, Madras-25*)

Received March 25, 1957

1. Introduction

The main features of the structure of collagen at the molecular level have been reasonably well worked out (Ramachandran and Kartha, 1955; 1956). The polypeptide chains form three non-coaxial helices in the protofibril and are further wound up into coiled coils about a common axis. The three chains are attached to one another by means of hydrogen bonds approximately perpendicular to the fibre axis. These triple chain rods are arranged in a hexagonal array, the distance between them varying with the amount of moisture present. Though this structure explains fairly well the wide angle X-ray pattern of collagen, some of the details are not yet clear. The most puzzling aspect is the non-occurrence of the $11\bar{2}0$ (110) reflection or its analogue having the same ξ-value in the higher layers. It is usually supposed that the Fourier transform of the structure is weak in this region, and that the absence of a spot in the zero layer corresponding to the 110 reflection is due to this cause; but it is difficult to believe that it should be so for every layer line. In fact, a spot having roughly this ξ-value ($\xi = 0{\cdot}20$) occurs on the fourth layer line of kangaroo tail tendon and was identified as such by Ramachandran and Ambady (1954). However, the actually observed ξ-value differs from the expected value of 0·24 by an appreciable amount. Thus it would appear that the whole series of reflections of the type $11l$ is forbidden for collagen. Further it is found that the observed ξ-values in general lie close to 0·14, 0·28 and 0·42 in all the layer lines, *i.e.*, in the ratio of 1 : 2 : 3 and not at intermediate values like $\sqrt{3}$ or $\sqrt{7}$ times the basic unit of 0·14. This suggests that reflections with mixed indices of the type hk (both h and k non-zero) do not occur in the X-ray pattern of collagen.

Although a few spacings larger than 15 Å have been previously reported (Corey and Wyckoff, 1936) they had not been confirmed. Photographs taken in this laboratory of native cattle achilles tendon showed diffuse maxima at about 18 Å, 29 Å and 46 Å. These agreed with the observations of Corey and Wyckoff. The publication of a beautiful photograph taken by Cowan, North and Randall (1955), recording a whole series of sharp reflections in

this range brought to light the fact that the earlier observations were done at insufficient resolution. Even in this photograph the 110 reflection is missing on the equator. The fact that such a large number of sharp reflections are observed at small angles shows that the specimen is well oriented and it is therefore all the more surprising that no reflections were recorded corresponding to the ξ-value of the 110 spacing of the hexagonal lattice.

This difficulty is resolved and at the same time the occurrence of a large number of equatorial long spacings is also explained, if it is assumed that the structure of collagen is not built on a regular lattice, but on a cylindrical lattice. The idea of cylindrical and spiral lattices is briefly discussed below and they are applied to the case of collagen. It is very probable that these concepts could be extended to other fibrous proteins as well; some suggestive evidence in these cases is also presented.

2. General Theory of Cylindrical Lattice

A number of excellent theoretical papers have appeared on cylindrical lattices, their classification and their Fourier transform (Whittaker, 1954; 1955; Jagodzinski and Kunze, 1954; Waser, 1954). We shall consider here briefly the general theory of a simple normal cylindrical lattice. Such a cylindrical lattice is built up of a series of sheets, forming the surfaces of coaxial cylinders, the radii of these increasing in arithmetical progression. In any small region, it could be imagined as having been derived from a regular lattice by giving it a cylindrical curvature. Thus if ρ_m is the radius of the m-th cylinder and p_m the number of lattice points along its circumference, then $\rho_m = a_0 + ma$, a_0 being the radius of the innermost cylinder and $2\pi\rho_m = p_m b$, where b is the distance between the neighbouring points along the circumference. Suppose that the z-axis is along the axis of the coaxial cylinders; then any point can be defined by the cylindrical co-ordinates ρ, ϕ and z. Let the points which are nearest to the initial plane ($\phi = 0$) lying on the m-th cylinder have the co-ordinates $\phi = \delta_m$. Then the angular parameters ϕ of the points in the m-th cylinder are given by

$$\phi = \frac{b\nu}{p_m} + \delta_m$$

where ν is an integer such that $1 \leqslant \nu \leqslant p_m$. Also $\rho = \rho_m = a_0 + ma$ and $z = nc$, where c is the repeat distance along the axis of the cylinder.

In accordance with the usual theory of diffraction, the amplitude of the diffracted wave along a direction given by the reciprocal vector **s** is the Fourier transform of these cylinders, which is given by

$$T = \sum_m \sum_n \sum_\nu \exp\left(\frac{2\pi i}{\lambda} \mathbf{r}.\mathbf{s}\right) \tag{1}$$

where $\mathbf{r}$ is the position vector. The vector $\mathbf{s}$ may be called the diffraction vector, whose terminus is given by the co-ordinates ρ^*, ϕ^* and z^*. Then,

$$\mathbf{r}.\mathbf{s} = \rho\rho^* \cos(\phi^* - \phi) - zz^* \tag{2}$$

Thus,

$$T = \sum_n \exp\left(\frac{2\pi i}{\lambda} ncz^*\right) \sum_m \sum_\nu \exp \frac{2\pi i}{\lambda} [\rho_{m\nu}\rho^* \cos(\phi^* - \phi_{m\nu})] \tag{3}$$

Replacing the exponential functions occurring in the sum in expression (3) by a series of Bessel functions,

$$T = \sum_n \exp\left(\frac{2\pi i}{\lambda} ncz^*\right) \sum_m \sum_{q=-\infty}^{\infty} i^q J_q\left(\frac{2\pi}{\lambda} \rho_{m\nu}\rho^*\right)$$

$$\times \exp[iq(\phi^* - \delta_m)] \sum_\nu \exp\left(-\frac{2\pi i q\nu}{p_m}\right) \tag{4}$$

The last sum, $\sum_\nu$, is finite only when $q = kp_m$ (where k is an integer) and it is then equal to p_m. It vanishes otherwise, so that,

$$T = \sum_n \exp\left(\frac{2\pi i}{\lambda} ncz^*\right) \sum_m p_m \sum_{q=-\infty}^{\infty} J_{kp_m}\left(\frac{2\pi}{\lambda} \rho_{m\nu}\rho^*\right)$$

$$\times \exp\left[ikp_m\left(\phi^* + \frac{\pi}{2} - \delta_m\right)\right] \tag{5}$$

The first summation, $\sum_n$, has appreciable values only in the vicinity of planes in the reciprocal space, given by $z^* = l\lambda/c$, where l is an integer. These are the usual layer lines. In the second summation, $\sum_m$, the square of the modulus of the functions, averaged over rapid oscillations in ϕ^*, causes all cross terms between high order Bessel functions associated with different values of k, and cross terms between them and J_0, to vanish. Also, cross terms involving different m's tend to vanish unless $k = 0$. Thus when $k \neq 0$ the intensity $|T|^2$ is proportional to

$$\sum_{k=1}^{\infty} \sum_m p_m^2 J_{kp_m}^2\left(\frac{2\pi}{\lambda} \rho_{m\nu}\rho^*\right) \tag{6}$$

This function has peaks corresponding to $\rho^* = k\lambda/b$ ($k = 1, 2, 3, \ldots$), thus leading to characteristic bands of large intensity in reciprocal space on

cylinders, whose radii are multiples of b^*. The intensity of the k-th band arises essentially from the Bessel functions of orders $\pm kp_m$. From the expression (6), it is seen that the intensities due to the scattering from the component cylinders of the lattice are additive for these bands. These bands are known as the 'diffuse' series, since they are accompanied by a tail of secondary maxima on the longer ρ^* side.

When $k = 0$, however, there is interference between the terms $J_0(2\pi/\lambda \times \rho_m\rho^*)$ for different ρ_m and the amplitudes due to the component cylinders are additive. The intensity $|T|^2$ is proportional to

$$\left| \sum_m p_m J_0\left(\frac{2\pi}{\lambda} \rho_m\rho^*\right) \right|^2 \tag{7}$$

The intensity exhibits sharp maxima on bands corresponding to $\rho^* = h\lambda/a$ (h integral).

Thus, the diffraction pattern can be described as consisting of a series of layer lines at $\xi = l\lambda/c$, on which two series of reflections occur, one the sharp series at $\xi = h\lambda/a$ (h integral) and the other the diffuse series at $\xi = k\lambda/b$.

The above discussion is confined to the case in which the two-dimensional lattice inscribed on the cylindrical layers is primitive and rectangular and has one axis oriented perpendicular to the cylinder axis. Whittaker (1955) has enumerated and classified the possible types of cylindrical lattices and has extended the theory to diffraction by regular cylindrical lattices, with an oblique generating lattice and by those belonging to the helical series. A particular case of diffraction by a helical structure has also been discussed by Jagodzinski and Kunze (1954). These papers may be consulted for a more detailed account of the theory.

3. CYLINDRICAL LATTICE FOR COLLAGEN

Let us consider a cylindrical lattice built up of protofibrils* all running parallel to the axis of the cylinders. Then in any cross-section the appearance will be similar to Fig. 1, in which each protofibril is represented by a small circle. The distance between successive cylinders is a and if b is the distance between the protofibrils on any cylinder, then we have the result $\Delta n = n_j - n_{j-1} = 2\pi a/b$, where n_j is the number of protofibrils on the j-th cylindrical surface. This must obviously be an integer and the number was chosen to be six for collagen. The choice came from a consideration of the symmetry of coupling the cylinders together, and the occurrence of a regular

* The term protofibril is used for the elementary unit of the structure. This may consist of a single polypeptide chain as in the α-helix or a triple chain, as in the collagen structure.

hexagonal lattice as an approximation. This immediately imposed a relation between a and b, namely, that $2\pi a = 6b$ and thereby the geometry of the structure was completely fixed.

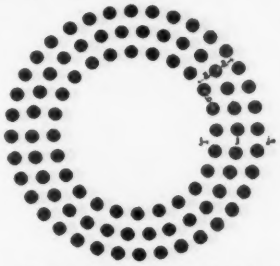

FIG. 1. Cross-section of a cylindrical lattice.

However, as one goes towards the centre, there are two possibilities in the central region, as indicated by Figs. 2 (*a*) and 2 (*b*). They are best described

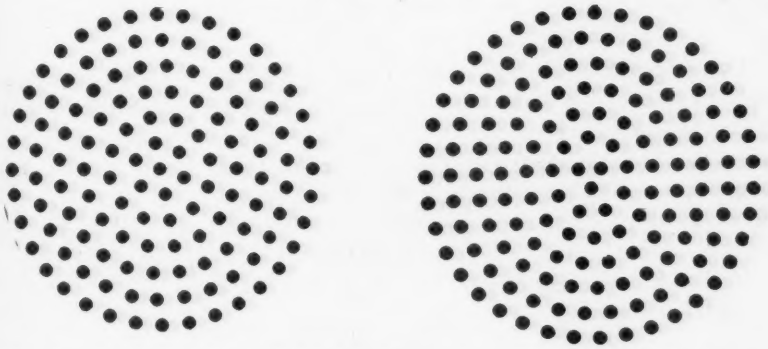

FIG. 2. The two possible cylindrical lattice structures of collagen. Each circle represents a protofibril. (*a*) Structure with one protofibril right at the centre. (*b*) Structure with three protofibrils forming an equilateral triangle at the centre.

by the relations (i) $a_j = ja$ and (ii) $a_j = (j - \frac{1}{2})\, a$. Thus Fig. 2 (*a*) has a protofibril right at the centre, while the innermost core in Fig. 2 (*b*) consists of three protofibrils forming an equilateral triangle. In both cases, the structure at the centre corresponds approximately to a regular hexagonal lattice and outside, it fits in with the scheme for a cylindrical lattice. The choice between the two could not be made on *a priori* grounds, but was possible from a detailed comparison with the equatorial long spacings in the X-ray pattern, which indicated that the structure shown in Fig. 2 (*b*) is the correct one. There is a reasonable fit with the data if the central protofibril is not there in the structure shown in Fig. 2 (*a*).

The c-axis of the structure was taken to be parallel to the cylinder axis, the repeat spacing being 28·6 Å, the value for the protofibril. From the properties of the transform of the cylindrical lattice, there will be maxima corresponding to $\xi = h\,\lambda/a = ha^*$ and $\xi = k\,\lambda/b = kb^*$ on the equator and on all layers defined by $\xi = l\,\lambda/c = lc^*$. In the present case, since $a/b = 2\pi/6 = 1{\cdot}047$, the two series of principal maxima (namely ha^* and kb^* series) practically coincide and only one set of principal reflections occur at $\xi = h\,\xi_0$ ($\xi_0 \simeq \lambda/a$). On the other hand, no reflections can occur at values of $\xi = ha^* + kb^*$, corresponding to mixed indices of the type h, k, with both h and k non-zero. Physically, this can also be explained as being due to the fact that, while there is a regular order among the points in any particular ring in Fig. 1 and also while the distance between any two circles is a constant, there is no correlation between the points in different circles in that figure. The points get in step and out of step periodically and so the analogue of a $hk0$ plane cannot occur.

Thus, while reflections of the type $h0l$ and $0kl$ are possible, those of the type $hk0$ and hkl cannot occur. In particular, 110 *is a forbidden reflection for collagen*, and this ξ-value cannot also occur in any of the layer lines. In fact, the absence of mixed h and k indices in the diffraction pattern of cylindrical lattices has been noticed in the case of chrysotile by Jagodzinski and Kunze (1954).

4. Comparison with the Observed Equatorial Long Spacings

The absence of the 110 reflection and its analogue in the other layers thus receives a natural explanation. However, the real evidence for the cylindrical lattice is obtained from a comparison of the calculated Fourier transform of the cylindrical lattice with the observed X-ray diffraction pattern. A number of subsidiary maxima occur at intermediate values of ξ in between the principal maxima. These have been worked out for the structure with seven cylindrical sheets [Fig. 2 (*b*)] and the results are shown in Table I for the region from 0 to ξ_0. The value of spacings larger than 10 Å observed on the equator and their relative intensities are given in columns 3 and 4 of Table I. The first and second columns contain the calculated spacings and intensities. The spacings were calculated taking the most intense reflection at 12·6 Å to correspond to the principal maximum of the first order. The number seven was arrived at by comparing the theoretical values with observations. The agreement between the calculated and observed values is seen to be good.

The sharpness of the observed maxima indicates that all the fibres in the specimen have exactly the same number of sheets. On drying the fibres,

TABLE I

Calculated and observed maxima in the diffraction pattern of a cylindrical lattice with 7 sheets

Calculated		Observed	
Spacing	Intensity (arbitrary units)	Spacing	Intensity
110	43·6	..	..
66	12·3	..	..
49·5	3·6	49·0	s
38	3·2	37·0	s
31·5	1·7	31·0	w
26·5	2·0	24·5	m
23·5	1·0		
20·5	1·8	20·5	w
18·5	1·0	18·8	m
16·8	3·2	17·0	m
15·4	2·9	14·9	m
13·9	38·0	13·5	v.s.
12·6*	93·0	12·6*	v.s.

* Adjusted to be equal.

this regularity is lost and on rewetting, only a streak joining the centre to the principal equatorial spots is observed. A similar streak is also observed in other layer lines, notably in the third layer line, showing that there is appreciable scattering power in the region in between the principal maxima. If the Fourier transform of the protofibril does not have a large value at the ξ-values corresponding to the principal maxima, but only in between, then it will record as a diffuse reflection on the particular layer line. The broad peak at $\xi = 0{\cdot}20$ in the fourth layer line is probably of this type.

In order to see the behaviour of the transform beyond the first principal maximum, the calculations were continued for the range from that to the second principal maximum for the structure with seven cylindrical sheets [Fig. 2 (*b*)]. From the cylindrical lattice theory, the intensity distribution along the equator, or zero layer, is given by

$$I(\xi) = c \left| \sum_{m=1}^{7} 3(2m-1)\, J_0\left(\pi(2m-1)\,\xi/a^*\right) \right|^2 + 2c\left[\sum_{k=1}^{\infty} \sum_{m=1}^{7} 9(2m-1)^2 J^2_{3k(2m-1)}\left(3(2m-1)\,\xi/b^*\right) \right]$$

where c is a constant. A graph is shown in Fig. 3 connecting intensity and the ξ-value. The intensity calculations were made at intervals of $\pi\ \xi/a^*$

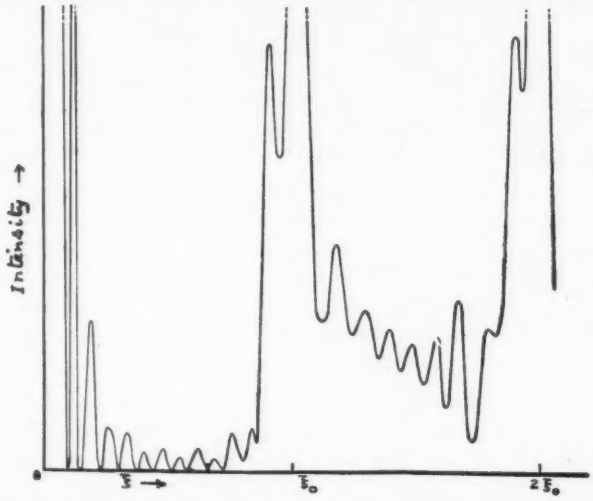

FIG. 3. A graph connecting the variation of intensity with ξ for the structure shown in Fig. 2 (*b*).

$= 3\xi/b^* = 0{\cdot}05$. The intensity variations in the range from 0 to ξ_0 ($\xi_0 \simeq \lambda/a$) is mainly due to the contribution by the first part of the above equation. The nature of the second function is such that it has appreciable values only when ξ approaches $k\ \xi_0$ and thereafter it is oscillatory in nature. The intensity however never falls to zero beyond ξ_0, so that sharp subsidiary maxima would not be observed. It must be noted that in general there is an appreciable scattering power in the region between any two principal maxima. This is a feature peculiar to the cylindrical lattice and does not occur with a regular lattice, even if the lattice is finite. With a finite regular lattice, the intensity distribution between any two principal maxima is the same and exhibits a number of subsidiary maxima, which fall away in intensity on moving away from a principal maxima. With a cylindrical lattice, this feature occurs only between zero and the first principal maxima. The diffuse intensity in the region between the principal maxima increases with increasing ξ-value.

There is thus clear evidence that the aggregation of collagen protofibrils is based on a cylindrical lattice and that they form cylindrical cryptofibrils of diameter approximately 200 Å [2× (13–15) × 7].† In fact fibrils of this

† The term "cryptofibril" is used to indicate cylindrical structures of the type discussed, with a diameter of the order of 200 Å.

order of diameter showing characteristic 640 Å axial period have been observed in the electron microscope. In particular, they are very clearly seen in the beautiful photographs reported by Swerdlow and Stromberg (1955) of fibrils subjected to mercury at high pressure. These pictures indicate that an ordinary fibril having a diameter of the order of 500–2000 Å is built up of such cryptofibrils. Burton *et al.* (1955) have found that fine threads, about 150–250 Å in diameter, are produced in the early stages of the degradation of collagen by chemical treatment.

5. The Possibility of Roll Structure

So far, we have discussed the cylindrical lattice structure. However, it seems physically more probable that a cylindrically curved layer structure would have for its cross-section a spiral, rather than a set of concentric circles. In that case, the complete structure can be obtained by rolling up a single sheet, in which the protofibrils form a parallel array.

In any cross-section, the equation to the spiral can be written in the form $r = k\theta$. As before, the whole structure can be characterised by two distances (i) the distance a between the sheets and (ii) the distance b between the protofibrils in the sheet. We may assume, to start with, that the sheet is rolled about an axis parallel to the protofibrils. If this were not so, the protofibrils would take up the configuration of a helix, whose radius is continuously increasing. So far, it has not been possible to work out theoretically the diffraction pattern of a spiral lattice, even of the simple type. However, by an experimental approach described in the next section, it is found that the rotated Fourier transform is of the same type as the one obtained from a cylindrical lattice.

The spiral lattice appropriate to collagen is shown in Fig. 4. Here also, the relation $2\pi a = 6b$ was used for plotting the lattice points. The lattice

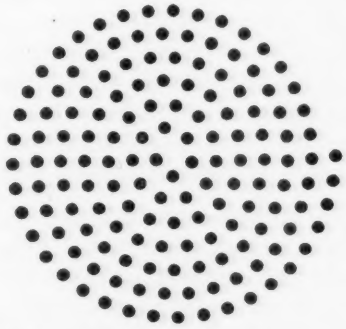

Fig. 4. Cross-section of a roll structure (spiral lattice) appropriate to collagen.

points were so plotted that the spiral structure thus obtained broadly resembled the one shown in Fig. 2 (*b*).

6. Optical Transforms of Cylindrical Lattice Structure of Collagen

The above results of the cylindrical and spiral lattice structures were confirmed by means of experiments, made on models with an optical diffractometer. The diffraction apparatus used in these experiments was the one described by Aravindakshan (1957). As with other optical diffraction apparatus, this also does not permit the study of diffraction patterns from three-dimensional objects. So investigations were carried out only of diffraction from plane circular and spiral lattices. However, for the present purpose, this does not involve any limitations, since the diffraction pattern obtained from such a lattice is equivalent to the distribution of intensity on the zero layer plane in reciprocal space for the corresponding cylindrical lattice.

The pinhole source used was 40 microns in diameter and the resolution was fairly high. Photographic etched masks (Aravindakshan, 1957) were used at the beginning of the experiment. Because of the non-uniformity of the photographic glass plate, distortions were produced in the image. A more serious difficulty was a displacement due to the non-parallelism of the two surfaces of the glass plate, as a result of which rotated optical transforms could not be recorded. The masks were later prepared using a pantograph punch on a scale 0·185 mm./Å. Each lattice point was represented by a hole 0·45 mm. in diameter. The first minimum of the diffraction pattern from a hole of this size occurs at $\xi = 0{\cdot}75$, which is well beyond the range ($\xi < 0{\cdot}30$) of the optical transform useful for study. These holes were punched on a blackened photographic film. The drawings, from which the masks were prepared, were constructed on a scale nine times larger. In order to plot the points of the lattice, their loci (either concentric circles or the spiral, as the case may be) were drawn first. The lattice points were then set off at equal distances along the curve, their positions being checked and corrected at least every 90°. The optical transforms were photographed directly on a fine grain photographic plate and enlarged for reproduction.

A comparison with the X-ray results can be best had when the transform is obtained with the mask continuously rotated in the optical diffraction apparatus. The transform thus obtained may be called ' rotated transform ' and for a satisfactory result, neither accurate centering of the mask nor absolute uniformity of motion is required. The only requirement is that

the plane of the mask must remain the same during rotation and this is readily achieved by using a good ball-bearing.

(*a*) *Cylindrical lattice.*—The optical transforms obtained for the two possible cylindrical lattice structures of collagen [(Figs. 2 (*a*) and 2 (*b*)] are shown in Figs. 5 and 6, along with their rotated transforms. The similarity between the two transforms is remarkable. In both cases, the six-fold symmetry of the pattern arises from the relation $2\pi a = 6b$. The sharpness of the maxima, their fine structure and the arch-like distribution of the diffuse reflections are all to be expected from theory.

The two rotated transforms contain rings of large intensity only at integral multiples of a unit and not at multiples like $\sqrt{3}$, $\sqrt{7}$, etc., which would be expected for a simple hexagonal lattice. The distinction between the cylindrical lattice and a simple hexagonal lattice of the same dimensions is easily seen by comparing their rotated transforms shown in Figs. 6 (*b*) and 7 (*b*). The absence of rings corresponding to the reflections 1, 1 and 2, 1 with the cylindrical lattice is particularly noteworthy and supports the theoretical prediction.

A number of weak rings (subsidiary maxima) are found in the rotated transform of the lattices, and are particularly clear in the central region inside the first ring. However, their number and spacings differ, *e.g.*, they are quite different for the two types of cylindrical lattice structures discussed here. In fact, it was the number and spacings of the subsidiary maxima near the central region which enabled the authors to choose the structure shown in Fig. 2 (*b*) as the proper one. The spacing of the rings for this structure are shown in Table II in the second column. The agreement between this and the observed spacings is seen to be good. In the photographs reproduced, only the stronger among the subsidiary maxima are clearly seen.

(*b*) *Spiral lattice.*—The optical transforms of the spiral lattice appropriate to collagen are shown in Fig. 8. The similarity between these and the transforms of the cylindrical lattices is striking; however, the symmetry is only approximately six-fold in this case. In the ordinary transform many of the spots making up the pattern do not lie in exactly the same positions on the various arches, a fact which clearly arises from the spiral character of the lattice.

As before, the rotated transform contains intense rings only at integral multiples of a unit. The spacings of the subsidiary maxima near the central region obtained from this lattice are given in Table II in the third column. The agreement between this and the observed spacings is again good. A

TABLE II

Observed spacings (in A*) in the X-ray diffraction pattern of collagen and the spacings calculated from measurements on the diffraction pattern of cylindrical and spiral lattices in an optical diffractometer*

From X-ray pattern	From rotated transform of	
	Cylindrical lattice	Spiral lattice
..	101	99
..	67	65
49·0	49·0	49
37·0	38·0	39
31·0	32·0	32
24·5	27·0	27
	24·0	23
20·5	21·0	20
18·8	..	..
17·0	17·0	17·3
14·9	15·4	14·8
13·5	14·2	14·0
12·6	12·6	12·6

comparison of the rotated transforms of the cylindrical and spiral lattices shows that there is more of intensity in between the principal maxima with the spiral lattice. This is to be expected, since there is less order in a spiral lattice than in a cylindrical lattice. The phenomenon is seen particularly well in the region between the first and second principal maxima in Fig. 8 (*b*). Thus all the evidences available so far are in accord with spiral lattice also, with the added advantage that the formation of a roll in the form of a continuous sheet is much more reasonable.

It is quite possible now that collagen has definitely been shown to have a cylindrical lattice structure, that other fibrous proteins also may have such a structure. This is particularly to be expected since the number of spots found in their X-ray pattern are very small, *e.g.*, in keratin, compared to those found in the patterns of some polypeptides. In fact, the published X-ray pattern of sea-gull feather keratin (Bear and Rugo, 1951) clearly indicates the occurrence of a cylindrical lattice. Only row lines corresponding to $h\,\xi_0$ are found with $h = 1, 2, 3, 4$ and $\xi_0 = 0{\cdot}045$. The absence of any other intermediate row lines of sharp spots clearly shows that a cylindrical lattice structure is present and also that the ratio a/b is probably the same as in

collagen. There is also an extension of reflecting power in some layer lines in between the principal row lines. Probably the α-keratin group also has this structure, as only one type of repeat spacing has been found along the equator.

Summary

It is suggested that the structure of collagen is based on a cylindrical lattice. The protofibrils, consisting of triple chains, are packed together in a hexagonal array close to the centre, and are extended outwards in the form of cylindrical sheets. Each sheet has a pseudohexagonal symmetry about the common axis. This cylindrical lattice explains (*a*) the large number of equatorial reflections of long spacings observed in the diffraction pattern of native fibres and (*b*) the absence of the 110 reflection and its analogue in all layer lines. The number of sheets in a single cylindrical rod is about 7 and its diameter about 200 Å.

The above results were verified by model optical diffraction experiments. Also, from these experiments it is shown that the structure can also belong to the roll type with the added advantage that the formation of a roll in the form of a continuous sheet is more probable from the point of view of fibrogenesis.

References

1. Aravindakshan, C. .. *J. Sci. Instrun.*, 1957 (in press).
2. Bear, R. S. and Rugo, H. J. *Ann. N.Y. Acad. Sci.*, 1951, **53**, 627.
3. Burton, D., Hall, D. A., Keech, M. K., Reed, R., Saxl, H. and Tuhbridge, R. E. *Nature*, 1955, **176**, 966.
4. Corey, R. B. and Wyckoff, R. W. G. *J. Biol. Chem.*, 1936, **114**, 407.
5. Cowan, P. M., North, A. C. T. and Randall, J. T. *Symp. Soc. Exptl. Biol.*, 1955, **9**, 115.
6. Jagodzinski, H. and Kunze, G. *Neues Jb. Miner. Mh.*, 1954, 95, 113, 137.
7. Ramachandran, G. N. and Ambady, G. K. *Curr. Sci.*, 1954, **23**, 349.
8. ——— and Kartha, G. .. *Proc. Ind. Acad. Sci.*, 1955, **42 A**, 215.
9. Ramachandran, G. N. .. *Nature*, 1956, **177**, 710.
10. Swerdlow, M. and Stromberg, R. R. *J. Res. Nat. Bur. Stds.*, 1955, **54**, 83.
11. Waser, J. .. *Acta Cryst.*, 1954, **8**, 142.
12. Whittaker, E. J. W. .. *Ibid.*, 1954, **7**, 827; 1955, **8**, 261, 265, 571, 726.

EXPLANATION OF PLATE X

FIG. 5. Transforms of the structure shown in Fig. 2 *a*. (*a*) Ordinary transform, (*b*) Rotated transform.

FIG. 6. Transforms of the structure shown in Fig. 2 *b*. (*a*) Ordinary transform, (*b*) Rotated transform.

FIG. 7. Transforms of a simple hexagonal lattice. (*a*) Ordinary transform, (*b*) Rotated transform.

FIG. 8. Transforms of the spiral lattice shown in Fig. 4. (*a*) Ordinary transform, (*b*) Rotated transform.

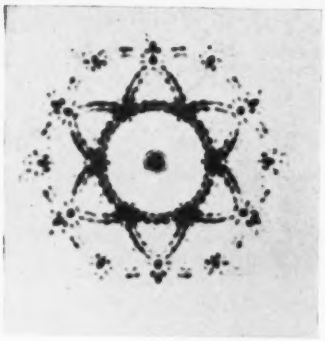

FIG. 5 (*a*)

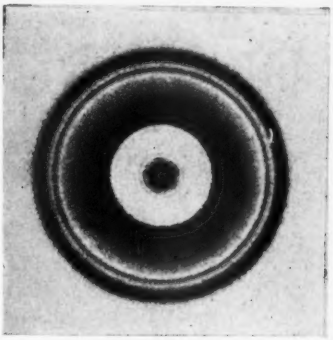

(*b*)

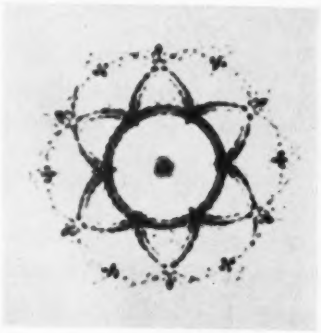

FIG. 6 (*a*)

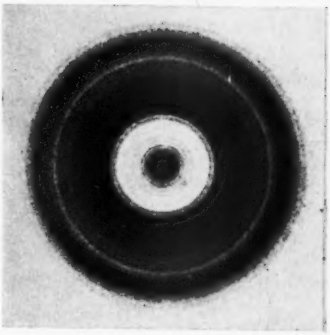

(*b*)

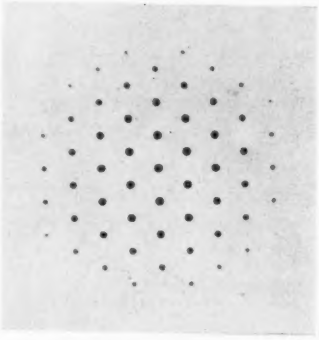

FIG. 7 (*a*)

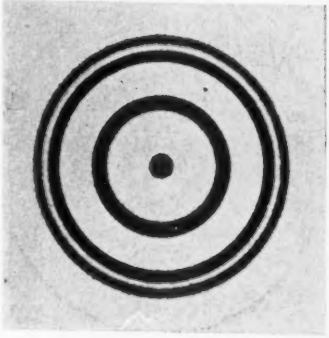

(*b*)

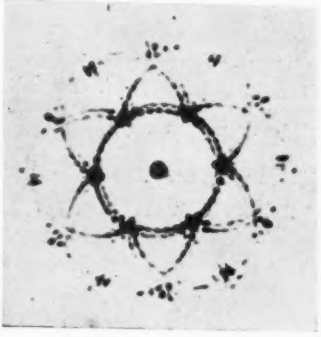

FIG. 8 (*a*)

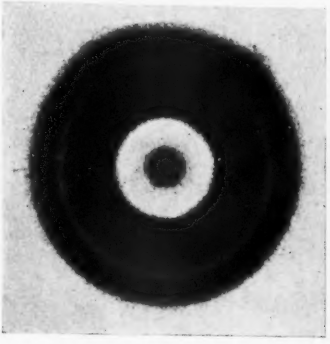

(*b*)

SOME APPLICATIONS OF BANACH FUNCTIONAL METHODS TO SUMMABILITY

By M. R. Parameswaran

(*Ramanujan Institute of Mathematics, Madras*)

Received April 2, 1957

(Communicated by Prof. B. S. Madhava Rac, F.A.SC.)

§ 1. Introduction

The matrix $A = (a_{ik})$, $i, k = 1, 2, 3, \ldots\ldots$ of real or complex constants transforms any given sequence $x = \{x_n\}$ of real or complex numbers into a sequence $y = \{A_i(x)\}$ by the equations

$$(T) \quad y_i \equiv A_i(x) = \sum_{k=1}^{\infty} a_{ik}x_k \qquad (i = 1, 2, 3, \ldots\ldots).$$

The sequence x is said to be summable by the matrix A to the value l if all the sums y_i are finite and $\lim_{i \to \infty} y_i = l$. We denote the transformation (T) by the matrix equation $y = Ax$, where y and x are column vectors whose elements in the i-th row are y_i and x_i respectively. For the sake of convenience we shall use the same symbol to represent a sequence and the column vector corresponding to it.

Let (c_0), (c) and (m) denote as usual the spaces of null sequences, convergent sequences and bounded sequences respectively, with the usual norm. If (X) and (Y) are two sets of sequences then (X) (Y) will denote their intersection, *i.e.*, the set of sequences (points) common to both (X) and (Y); and we shall denote by $\Gamma(X, Y)$ the class of all matrices A which have the property that $x \in (X)$ implies $Ax \in (Y)$. We define further, for every complex number ρ that $\Gamma(c, \rho c)$ is the class of matrices A such that $\lim_{i \to \infty} x_i = l$ implies $\lim_{i \to \infty} \sum_{k=1}^{\infty} a_{ik}x_k = \rho l$. Therefore in particular $\Gamma(c, c)$ is the set of all K-matrices (conservative or convergence-preserving matrices) and $\Gamma(c, 1c)$ is the set of all T-matrices (permanent or regular matrices).

The summability field of A, *i.e.*, the set of all sequences $x = \{x_n\}$ such that $Ax \in (c)$ will be denoted by the symbol (A), and if (X) is a given set of sequences, we define $R_{(X)}(A)$ to be the " range of A over (X) ", *i.e.*, as the set of sequences y such that $y = Ax$ where $x \in (X)$.

The object of this paper is to extend some results that Banach [(1), pp. 90–95] has proved for $\Gamma(c, 1c)$ to other classes of matrices and to derive therefrom a number of other theorems. The immediate extensions of Banach's results and the extensions obtained therefrom of some results due respectively to Hanai (3), Hill (4) and Ramanujan (7) are given in § 2; in § 3 we show that applications of these functional analysis methods and result yield a number of theorems due respectively to Copping (2), Wilansky (8) and the author (5), (6). The proofs as well as some of the results of § 3 are believed to be also new.

§ 2

We begin by recalling that the necessary and sufficient conditions in order that the matrix A should belong to (*i*) $\Gamma(m, m)$, (*ii*) $\Gamma(c, c)$, (*iii*) $\Gamma(c_0, c_0)$, (*iv*) $\Gamma(c, \rho c)$ are, respectively,

(i) (*a*): $\| A \| \equiv \underset{1 \leqslant i < \infty}{l.\,u.\,b.} \sum_{k=1}^{\infty} | a_{ik} | < \infty$

(ii) (*a*) is satisfied,

(*b*): $\lim_{i \to \infty} \sum_{k=1}^{\infty} a_{ik} = \rho$ exists, and

(*c*): $\lim_{i \to \infty} a_{ik} = \delta_k$ exists for each $k = 1, 2, 3, \ldots$.

(iii) (*a*) and (*c*) are true, with $\delta_k = 0$ for all $k = 1, 2, 3, \ldots$.

(iv) (*a*), (*b*) and (*c*) are true, with $\delta_k = 0$ for all $k = 1, 2, 3, \ldots$.

THEOREM 1.1[1].—*If the matrix* $A \epsilon \Gamma(c, c)$ *satisfies the condition*

$$\chi(A) \equiv \lim_{i \to \infty} \sum_{n=1}^{\infty} a_{in} - \sum_{n=1}^{\infty} \lim_{i \to \infty} a_{in} \equiv \rho - \sum_{n=1}^{\infty} \delta_n \neq 0 \qquad (2.1)$$

and if $y = \{y_i\}$ is a convergent sequence such that

$$\sum_{i=1}^{\infty} a_i y_i = 0 \qquad (2.2)$$

whenever

$$\sum_{i=1}^{\infty} | a_i | < \infty \text{ and } \sum_{i=1}^{\infty} a_i a_{in} = 0 \text{ for all } n = 1, 2, 3, \ldots. \qquad (2.3)$$

[1] Banach [(1), p. 91] has proved this theorem for the case $A \epsilon \Gamma(c, 1c)$ when (2.1) is automatically satisfied.

then there exists for every number $\epsilon > 0$ *a convergent sequence* x *such that*

$$|\, A_i(x) - y_i \,| < \epsilon \text{ for all } i = 1, 2, 3, \ldots. \tag{2.4}$$

PROOF.—The conclusion of the theorem means that $y \epsilon \overline{R_{(c)}(A)}$, where $\overline{R_{(c)}(A)}$ is the closure of the set of A-transforms of convergent sequences. By a lemma of Banach [(1), p. 57] it is plainly enough to prove that every linear continuous functional[2] vanishing over $R_{(c)}(A)$ will vanish at y. Now, any linear continuous functional defined over (c) is of the form [(1), p. 66].

$$f(s) = c_0 s_0 + \sum_{n=1}^{\infty} c_n s_n, \quad |\, c_0 \,| + \sum_{n=1}^{\infty} |\, c_n \,| < \infty \tag{2.5}$$

where $s = \{s_n\}$ has s_0 for limit. Therefore any linear continuous functional over $R_{(c)}(A)$ will be of the form

$$f(v) = f(Au) = c_0 [\rho u_0 + \Sigma\, \delta_p (u_p - u_0)] + \sum_{n=1}^{\infty} c_n \sum_{p=1}^{\infty} a_{np} u_p \tag{2.6}$$

where $u = \{u_i\}$ and $\lim_{i \to \infty} u_i = u_0$. Using the condition (2.1) and (ii) (a), we may write

$$f(v) = \sum_{p=1}^{\infty} u_p b_p + c_0 u_0\, \chi(A)$$

where

$$b_p = c_0 \delta_p + \sum_{n=1}^{\infty} c_n a_{np} \text{ for all } p = 1, 2, 3, \ldots. \tag{2.7}$$

Now if the functional f vanishes over $R_{(c)}(A)$, then taking $u^{(n)} = \{\delta_i^{\,n}\}$, where $\delta_i^{\,n}$ has the value unity if $i = n$ and is zero otherwise, for $n = 1, 2, 3, \ldots$. successively, we see that

$$b_p = 0 \text{ for all } p = 1, 2, 3, \ldots. \tag{2.8}$$

Therefore form (2.6) it follows that $f(v) = c_0 u_0\, \chi(A) = 0$.

Since by hypothesis $\chi(A) \neq 0$, we see by taking $u^{(0)} = \{\delta_i^{\,i}\}$ that $c_0 = 0$. The equations (2.7) and (2.8) now give

$$\sum_{n=1}^{\infty} c_n a_{np} = 0 \text{ for all } p = 1, 2, 3, \ldots.$$

---

[2] We prefer this terminology to Banach's "linear functional" in order to avoid any possible confusion.

and since by (2.5) $\sum_{n=1}^{\infty} | c_n | < \infty$ it follows from the hypothesis that $\sum_{n=1}^{\infty} c_n y_n = 0$ and therefore $f(y) = c_0 \lim_{i \to \infty} y_i + \sum_{n=1}^{\infty} c_n y_n = 0$. This proves the theorem.

A trivial modification of the proof of Theorem 1.1 gives the following:

THEOREM 1.2.—*If* $A \epsilon \Gamma(c_0, c_0)$ *and* $y \epsilon (c_0)$ *are such that* (2.3): $\sum_{i=1}^{\infty} | a_i | < \infty$, $\sum_{i=1}^{\infty} a_i a_{in} = 0$ *for all* $n = 1, 2, \ldots$ *implies* (2.2): $\sum_{i=1}^{\infty} a_i y_i = 0$, *then there exists for every number* $\epsilon > 0$ *a null sequence* x *such that* $| A_i(x) - y_i | < \epsilon$ *for all* $i = 1, 2, 3, \ldots\ldots$

THEOREM 2.—(Generalised converse of Theorem 1.1.)[3]

Let $A \epsilon \Gamma(m, m)$ *and* $y = \{y_i\}$ *be such that for every* $\epsilon > 0$ *there exists a sequence* $x \epsilon (m)$ *satisfying the condition*

$$| A_i(x) - y_i | < \epsilon \text{ for all } i = 1, 2, 3, \ldots\ldots$$

Then for any sequence $\{a_i\}$ *such that*

$$\sum_{i=1}^{\infty} |a_i| < \infty \text{ and } \sum_{i=1}^{\infty} a_i a_{in} = 0 \text{ for all } n = 1, 2, 3, \ldots. \quad (2.3)$$

we shall have

$$\sum_{i=1}^{\infty} a_i y_i = 0.$$

PROOF.—Let $\{a_i\}$ be a sequence satisfying the condition (2.3). Then $\alpha(s) \equiv \sum_{i=1}^{\infty} a_i s_i$ is a linear continuous functional defined over (m) and $\| \alpha \| = \sum_{i=1}^{\infty} | a_i |$. Also, $y \epsilon (m)$ since $Ax = \{A_i(x)\} \epsilon (m)$ and therefore we have:

$$| \alpha (Ax - y) | = | \sum_{i=1}^{\infty} a_i (\sum_{n=1}^{\infty} a_{in} x_n - y_i) |$$
$$\leqslant \| \alpha \| \cdot \| Ax - y \| < \| \alpha \| \cdot \epsilon \quad (2.9)$$

and since $\sum_{i=1}^{\infty} \sum_{n=1}^{\infty} | a_i | \cdot | a_{in} | \cdot | x_n | \leqslant \| \alpha \| \cdot \| A \| \cdot \| x \| < \infty$

we have

$$\alpha(Ax) = \sum_{i=1}^{\infty} a_i \sum_{n=1}^{\infty} a_{in} x_n$$
$$= \sum_{n=1}^{\infty} x_n \sum_{i=1}^{\infty} a_i a_{in}$$
$$= 0 \text{ by } (2.3).$$

[3] Hanai (3) has proved this theorem for the case $A \epsilon \Gamma(c, 1c)$. The proof given here is simpler.

Therefore (2.9) gives

$$|\sum_{i=1}^{\infty} a_i y_i| \leqslant |a(Ax - y)| + |a(Ax)| < \|a\| \cdot \epsilon. \quad \text{Since } \epsilon > 0$$

is as small as we please, we see that $\sum_{i=1}^{\infty} a_i y_i = 0$.

DEFINITION.—If the matrix A is such that for every sequence $\{a_i\}$ the condition (2·3) implies that $a_i = 0$ for all $i = 1, 2, 3, \ldots$, then A is said to be of *type M*.

THEOREM 3·1.[4]—*Let* $A \epsilon \Gamma(c, c)$ *be of type M and let* $\chi(A) \neq 0$. *Then* $R_{(c)}(A)$ *is dense in* (c).

The proof is immediate after Theorem 1.1.

As a consequence of Theorems 1·2 and 2 we have the

THEOREM 3·2.[5]—*The matrix* $A \epsilon \Gamma(c_0, c_0)$ *is of type M if and only if* $R_{(c_0)}(A)$ *is dense in* (c_0).

THEOREM 3.3.—*Let* $A \epsilon \Gamma(m, m)$. *Then* $R_{(c)}(A)$ *is dense in* (c) *if and only if the set of sequences (points) consisting of the columns of the matrix A and the sequence of row-sums* $\{\sum_{n=1}^{\infty} a_{in}\}$ *is fundamental in* (c).

PROOF.—If we denote by $\triangle$ the linear space generated by the set of sequences $\{\delta_i^{(n)}\}$, $n = 0, 1, 2, \ldots$, where $\delta_i^{(n)} = 1$ or 0 according as $i = n$ or $i \neq n$ for $n > 0$ and $\delta_i^{(0)} = 1$ for all i, then it is well known that $\overline{\triangle}$ is (c). Now, the linear space generated by the set mentioned in the theorem is the same as the set $R_{\triangle}(A)$. Since $\overline{\triangle}$ is (c) and since A defines a linear continuous operation over the Banach space (m) [in virtue of (1), Theoreme 1, p. 54] and the relations $l.u.b._{1 \leqslant i < \infty} |\sum_{n=1}^{\infty} a_{in} x_n| \leqslant l.u.b._{1 \leqslant i < \infty} \sum_{n=1}^{\infty} |a_{in}| \cdot l.u.b._{1 \leqslant n < \infty} |x_n| = \|A\| \cdot \|x\|$

it follows that $\overline{R_{\triangle}(A)} \supset R_{(c)}(A)$. Therefore we have:

$$\overline{R_{\triangle}(A)} = \overline{\overline{R_{\triangle}(A)}} \supset \overline{R_{(c)}(A)}.$$

---

[4] Banach [(1), p. 93] has proved this for $A \epsilon \Gamma(c, 1c)$ when the condition $\chi(A) \neq 0$ is automatically satisfied.

[5] It may be remarked that Ramanujan (7) has proved this theorem for $A \epsilon \Gamma(c, 1c)$ without however making use of the condition (ii) (*b*) of §2.

But $R_{\triangle}(A) \subset R_{(c)}(A)$ and hence we see that $\overline{R_{\triangle}(A)} = \overline{R_{(c)}(A)}$. This proves the theorem.

By arguing in exactly the same manner we get the result: *Let* $A \in \Gamma(m, m)$. *Then* $R_{(c_0)}(A)$ *is dense in* (c_0) *if and only if the columns of* A *form a set fundamental in* (c_0). Theorem 3·2 now yields the following:

THEOREM 3·4.—*The matrix* $A \in \Gamma(c_0, c_0)$ *is of type M if and only if its columns form a set fundamental in* (c_0).

THEOREM 4.—(Generalised converse of Theorem 3·1.)

If $A \in \Gamma(m, m)$ *and* $R_{(m)}(A)$ *is dense in* (c_0) *then* A *is of type M.*

PROOF.—Since $\overline{R_{(m)}(A)} \supset (c_0)$ we see that for every $y \in (c_0)$ and every number $\epsilon > 0$ there exists a bounded sequence x such that

$$| A_i(x) - y_i | < \epsilon \text{ for all } i = 1, 2, 3, \ldots .$$

In virtue of Theorem 2, the condition (2·3) will then imply that $\sum_{i=1}^{\infty} a_i y_i = 0$.

Since this is true for every null sequence y, we see by considering the sequences $y^{(n)} = \{\delta_i^{(n)}\}$, $n = 1, 2, 3, \ldots$ that $a_i = 0$ for all $i = 1, 2, 3, \ldots$ and the theorem is proved.

COROLLARY.[6]—*The matrix* $A \in \Gamma(c, c)$, $\chi(A) \neq 0$, *is of type M if and only if* $R_{(c)}(A)$ *is dense in* (c).

THEOREM 5·1.—*If* $A \in \Gamma(c_0, c_0)$, *then for every bounded sequence* x_0 *such that* $Ax_0 \in (c_0)$ *and for every number* $\epsilon > 0$ *there exists a null sequence* x *satisfying the condition*

$$| A_i(x) - A_i(x_0) | < \epsilon \text{ for all } i = 1, 2, 3, \ldots .$$

In other words, *if* $A \in \Gamma(c_0, c_0)$ *then* $R_{(c_0)}(A)$ *is dense in* $R_{(A_0)(m)}(A)$, *where* (A_0) *denotes the set of sequences which are summable by* A *to the value* 0.

PROOF.—Let us write $y_i = A_i(x_0)$ for each $i = 1, 2, 3, \ldots$ and let $\{a_i\}$ be a sequence such that $\sum_{i=1}^{\infty} | a_i | < \infty$ and $\sum_{i=1}^{\infty} a_i a_{in} = 0$ for all $n = 1, 2, 3, \ldots$. We have then

[6] Hill (4) has proved this for reversible matrices in $\Gamma(c, 1c)$ though he does not seem to use the reversibility.

$$\sum_{i=1}^{\infty} a_i y_i = \sum_{i=1}^{\infty} a_i A_i(x_0) = \sum_{i=1}^{\infty} a_i \sum_{n=1}^{\infty} a_{in} s_n$$

$$= \sum_{n=1}^{\infty} s_n \sum_{i=1}^{\infty} a_i a_{in} = 0$$

(the order of summation being justified by the fact that $\sum_{i=1}^{\infty} \sum_{n=1}^{\infty} |a_i| \cdot |a_{in}| \cdot |s_n| \leqslant \sum_{i=1}^{\infty} |a_i| \cdot \|A\| \cdot \|s\| < \infty$).

The result follows now from Theorem 1.2.

THEOREM 5.2.[7]—*If* $A \epsilon \Gamma(c, c)$ *and* $\chi(A) \neq 0$ *then* $R_{(c)}(A)$ *is dense in* $R_{(A)(m)}(A)$.

PROOF.—Same as for Theorem 5.1, only at the end we use Theorem 1.1 instead of Theorem 1.2.

THEOREM 5.3.—*Let* $A \epsilon \Gamma(m, m)$ *and let there exist for every number* $\epsilon > 0$ *and for every given* $x_0 \epsilon (A)(m)$ *a sequence* x *such that*

$$|A_i(x) - A_i(x_0)| < \epsilon \text{ for all } i = 1, 2, 3, \ldots.$$

Then for any sequence satisfying (2.3) *we shall have* $\sum_{i=1}^{\infty} a_i A_i(x_0) = 0$.

PROOF.—We have only to write $y = \{y_i\} = \{A_i(x_0)\}$ and apply Theorem 2.

§ 3

In this Section we apply the results obtained above to reciprocals of summability matrices.

THEOREM 6.1.—*Let* $A \epsilon \Gamma(c, c)$, $\chi(A) \neq 0$ *and let* $'A \epsilon \Gamma(m, m)$ *where* $'A.A = I$, *the identity. Then* $(A)(m) = (c)$.

PROOF.—We note that $'A$ sums every $x \epsilon R_{(c)}(A)$ for $'A(Au) = u$ for all $u \epsilon (c)$, indeed for all $u \epsilon (m)$. Now, by Theorem 5.2, $R_{(c)}(A)$ is dense in $R_{(A)(m)}(A)$; also, since $'A \epsilon \Gamma(m, m)$ we see that $'A$ defines a linear continuous operation over (m) by a well-known result [Banach (1), Theorème 1, p. 54]. Therefore it follows that $'A$ sums every $x \epsilon R_{(A)(m)}(A)$. That is, if $y \epsilon (A)(m)$ and $x = Ay$ then $'Ax = 'A(Ay) = y$ belongs to (c). It follows that $(A)(m) \subset (c)$ and since $A \epsilon \Gamma(c, c)$ the theorem is proved.

THEOREM 6.2.[8]—*If* $A \epsilon \Gamma(c, c)$ *and* $\chi(A) = 0$, *then there is no matrix* $'A \epsilon \Gamma(m, m)$ *such that* $'A.A = I$.

[7] Banach [(1), p. 93] has proved this for the special case $A \epsilon \Gamma(c, 1\ c)$.

[8] This result has recently been announced by Wilansky (8).

PROOF.—It is well known that under the hypothesis of the theorem there exists a bounded divergent sequence summable by the method A, *i.e.*, $(A)(m) \neq (c)$. The required result now follows from Theorem 6·1.

THEOREM 6·3.[9]—*If* $A \epsilon \Gamma(c, c)$ *and* $'A \epsilon \Gamma(m, m)$, $'A \cdot A = I$, *then* $(A)(m) = (c)$.

PROOF.—This follows immediately from Theorems 6·1 and 6·2.

THEOREM 6·4.[10]—*If* $A \epsilon \Gamma(c, c)$ *and* $A^{-1} \epsilon \Gamma(m, m)$ *is such that* $A^{-1} \cdot A = A \cdot A^{-1} = I$, *then* $A^{-1} \epsilon \Gamma(c, c)$.

PROOF.—Let $x = \{x_n\}$ be any convergent sequence. Then $A(A^{-1}x) = x \epsilon (c)$. Theorem 6·3 gives now that $A^{-1}x \epsilon (c)$. Since this is true for all $x \epsilon (c)$, the theorem is proved.

THEOREM 6·5.—*If* $A \epsilon \Gamma(c_0, c_0)$ *and* $'A \epsilon \Gamma(m, m)$, $'A \cdot A = I$, *then* $(A_0)(m) = (c_0)$.

The proof is the same as that for Theorem 6·1, only read (c_0) wherever (c) occurs and use Theorem 5·1 instead of Theorem 5·2.

THEOREM 6·6.—*If* $A \epsilon \Gamma(c_0, c_0)$ *and* $A^{-1} \epsilon \Gamma(m, m)$ *is such that* $A^{-1} \cdot A = A \cdot A^{-1} = I$, *then* $A^{-1} \epsilon \Gamma(c_0, c_0)$.

The proof follows from Theorem 6·5 just as Theorem 6·4 followed from Theorem 6·3.

REFERENCES

1. Banach, S. .. *Theorie des Operations Lineaires*, Warsaw, 1932.
2. Copping, J. F. .. "K-matrices which sum no bounded divergent sequences," *Journ. London Math. Soc.*, 1955, **30**, 123–27.
3. Hanai, S. .. "On the methods of summation of infinite series," *Tohoku Math. Jour.*, 1950, **2**, 64–67.
4. Hill, J. D. .. "On perfect methods of summability," *Duke Math. Journ.*, 1937, **3**, 702–14.
5. Parameswaran, M. R. .. "On the reciprocal of a K-matrix," *Journ. Indian Math. Soc.* (To appear).
6. ———— .. "Note on a theorem of Mazur and Orlicz in summability" (To appear).
7. Ramanujan, M. S. .. "On summability methods of type M," *Journ. London Math. Soc.*, 1954, **29**, 184–89.
8. Wilansky, A. .. "The inverse matrix in summability (Abstract)," *Bull. American Math. Soc.*, 1956, **26**, 252.

[9] See Copping (2) and Parameswaran (6) for two other proofs of this theorem.

[10] See Parameswaran (5) for a different proof of this theorem.

ON SUMS INVOLVING THE FRACTIONAL PARTS OF NUMBERS

By S. Swetharanyam

(*Department of Mathematics, Annamalai University*)

Received March 25, 1957

(Communicated by Prof. B. S. Madhava Rao, F.A.SC.)

Certain results regarding the asymptotic values of sums involving the fractional parts of numbers have been proved and made use of by Pillai and Chowla[3] in some other connection. Here we shall prove three theorems about sums involving the fractional parts of numbers, but of a different type. Throughout this paper $\{x\}$ denotes the fractional part of x and $[x]$ denotes the integral part of x, where x is any positive real number.

Theorem 1: $\sum_{d=1}^{x} \left\{\frac{x}{d}\right\} = (1-\gamma)\,x + 0\,(x^{\frac{1}{2}})$, *where* γ *is Euler's constant.*

Theorem 2: $\sum_{d=1}^{x} d \left\{\frac{x}{d}\right\} = \left(1 - \frac{\pi^2}{12}\right) x^2 + 0\,(x \log x)$.

Theorem 3: $\sum_{d=1}^{x} d^k \left\{\frac{x}{d}\right\} = \left(\frac{1}{k} - \frac{\zeta(k+1)}{k+1}\right) x^{k+1} + 0\,(x^k)$, *for all* $k \geqslant 2$, *where* $\zeta(s)$ *is the Riemann Zeta Function.*

Proof of Theorem 1: We have

$$\sum_{n=1}^{x} d(n) = x \log x + (2\gamma - 1)\,x + 0\,(x^{\frac{1}{2}}), \qquad (1)$$

(*vide* Hardy and Wright,[1] Theorem 320), where $d(n)$ is the number of positive divisors of n including 1 and n. From the definition of $d(n)$ we have

$$d(n) = \sum_{d \mid n} 1.$$

Hence

$$\sum_{n=1}^{x} d(n) = \sum_{n=1}^{x} \sum_{d \mid n} 1$$

$$= \sum_{dd' \leqslant x} 1 \text{ which is the same as}$$

$$\sum_{n=1}^{x} d(n) = \sum_{d=1}^{x} \sum_{d'=1}^{[x/d]} 1$$

$$= \sum_{d=1}^{x} \left[\frac{x}{d}\right]$$

$$= \sum_{d=1}^{x} \left(\frac{x}{d} - \left\{\frac{x}{d}\right\}\right)$$

$$= x\left(\log x + \gamma + 0\left(\frac{1}{x}\right)\right) - \sum_{d=1}^{x} \left\{\frac{x}{d}\right\}, \tag{2}$$

since

$$\sum_{n=1}^{x} \frac{1}{n} = \log x + \gamma + 0\left(\frac{1}{x}\right).$$

From (1) and (2) we have the theorem.

PROOF OF THEOREM 2: We have

$$\sum_{n=1}^{x} \sigma(n) = \frac{\pi^2 x^2}{12} + 0(x \log x), \tag{3}$$

(*vide* HARDY and WRIGHT,[1] Theorem 324). Here $\sigma(n)$ is defined as the sum of the positive divisors of n including 1 and n, and so

$$\sigma(n) = \sum_{d|n} d.$$

Hence

$$\sum_{n=1}^{x} \sigma(n) = \sum_{n=1}^{x} \sum_{d|n} d$$

$$= \sum_{dd' \leqslant x} d$$

$$= \sum_{d=1}^{x} d \sum_{d'=1}^{[x/d]} 1$$

$$= \sum_{d=1}^{x} d\left(\frac{x}{d} - \left\{\frac{x}{d}\right\}\right)$$

$$= x \cdot x - \sum_{d=1}^{x} d \left\{\frac{x}{d}\right\}. \tag{4}$$

So from (3) and (4) Theorem 2 follows.

To prove Theorem 3 we shall require the following lemmas:

LEMMA 1: (The Euler-Mclaurin sum formula in its simplest form, *vide* KNOPP,[2] p. 539.)

If f(x) *is continuous and differentiable for all values of* x, *then*

$$\sum_{n=0}^{x} f(x) = \int_{0}^{n} f(x)\,dx + \tfrac{1}{2}\left(f(0) + f(n)\right)$$

$$+ \int_{0}^{n} (x - [x] - \tfrac{1}{2}) f'(x)\,dx.$$

Applying the above lemma to the case when

$$f(x) = \frac{1}{(x+1)^a}, \quad a < 0, \text{ we have}$$

LEMMA 2:

$$\sum_{n=1}^{n} \frac{1}{x^a} = \frac{n^{1-a}}{1-a} + 0(n^{-a}), \quad a < 0.$$

PROOF OF THEOREM 3: As usual, let us denote by $\sigma_k(n)$ the sum of the k-th powers of the positive divisors of n including 1 and n, for all $k \geqslant 2$. So we have

$$\sigma_k(n) = \sum_{d|n} d^k.$$

We shall now estimate $\sum_{n=1}^{x} \sigma_k(n)$ in two different ways. Firstly,

$$\begin{aligned}
\sum_{n=1}^{x} \sigma_k(n) &= \sum_{n=1}^{x} \sum_{d|n} d^k \\
&= \sum_{dd' \leqslant x} d^k \\
&= \sum_{d=1}^{x} d^k \sum_{d'=1}^{[x/d']} 1 \\
&= \sum_{d=1}^{x} d^k \left(\frac{x}{d} - \left\{\frac{x}{d}\right\}\right) \\
&= x \sum_{d=1}^{x} \frac{1}{d^{1-k}} - \sum_{d=1}^{x} d^k \left\{\frac{x}{d}\right\}.
\end{aligned}$$

Since $1 - k < 0$, using Lemma 2 in the right side of the above, we have

$$\begin{aligned}
\sum_{n=1}^{x} \sigma_k(n) &= x\left(\frac{x^k}{k} + 0(x^{k-1})\right) - \sum_{d=1}^{x} d^k \left\{\frac{x}{d}\right\} \\
&= \frac{1}{k} x^{k+1} + 0(x^k) - \sum_{d=1}^{x} d^k \left\{\frac{x}{d}\right\}. \qquad (5)
\end{aligned}$$

Next we have

$$\begin{aligned}
\sum_{n=1}^{x} \sigma_k(n) &= \sum_{dd' \leqslant x} d^k \\
&= \sum_{d'=1}^{x/2} 1 \sum_{d=1}^{[x/d']} d^k + \sum_{d'=x/2}^{x} 1 \sum_{d=1}^{[x/d]} d^k \\
&= S + S' \text{ (say)}.
\end{aligned}$$

Since $-k<0$, by Lemma 2 we have

$$S=\sum_{d'=1}^{x/2}\left(\frac{[x/d']^{1+k}}{1+k}+0\left([x/d']^{k}\right)\right).$$

But

$$\left[\frac{x}{d'}\right]^{\alpha}=\left(\frac{x}{d'}-\epsilon\right)^{\alpha},\ 0\leqslant\epsilon<1$$

$$=\left(\frac{x}{d'}\right)^{\alpha}\left(1-\frac{\epsilon d'}{x}\right)^{\alpha}$$

and in

$$1\leqslant d'\leqslant\frac{x}{2}$$

$\frac{d'}{x}\leqslant\frac{1}{2}$ and so

$$\frac{\epsilon d'}{x}<\frac{1}{2}$$

uniformly and so

$$\left[\frac{x}{d'}\right]^{\alpha}=\left(\frac{x}{d'}\right)^{\alpha}\left\{1+0\left(\frac{d'}{x}\right)\right\}.$$

Hence

$$S=\sum_{d'=1}^{x/2}\left[\frac{(x/d')^{k+1}}{k+1}+0\left(\left(\frac{x}{d'}\right)^{k}\right)\right]$$

$$=\frac{x^{k+1}}{k+1}\sum_{d'=1}^{x/2}\frac{1}{d'^{k+1}}+0\left(x^{k}\sum_{d'=1}^{x/2}\frac{1}{d'^{k}}\right).$$

Since $k>1$, using the expression for the Riemann Zeta Function for the sums in the above, we have

$$S=\frac{x^{k+1}}{k+1}\left(\zeta(k+1)+0\left(x^{-k}\right)\right)+0\left(x^{k}\right)\left(\zeta(k)+0\left(x^{1-k}\right)\right)$$

$$=\frac{\zeta(k+1)}{(k+1)}x^{k+1}+0\left(x^{k}\right).$$

Now in $x/2\leqslant d'\leqslant x$, $x/d'\leqslant 2$ and hence in the sum $\sum_{d=1}^{[x/d']}d^{\alpha}$, there are atmost two terms. So we have $\sum_{d=1}^{[x/d']}d^{\alpha}=0(1)$ for any α, when $x/2\leqslant d'\leqslant x$,

Hence

$$S' = 0\left(\sum_{d'=a/2}^{a} 1\right)$$

$$= 0(x).$$

Hence

$$\sum_{n=1}^{a} \sigma_k(n) = S + S'$$

$$= \frac{\zeta(k+1)}{(k+1)} x^{k+1} + 0(x^k) + 0(x)$$

$$= \frac{\zeta(k+1)}{(k+1)} x^{k+1} + 0(x^k). \qquad (6)$$

Now equating the right sides of (**5**) and (**6**), we get the theorem.

Finally, I wish to thank Professor V. Ganapathi Iyer for his valuable advice in the preparation of this paper.

References

1. Hardy, G. H. and Wright, E. M. — *An Introduction to the Theory of Numbers*, 3rd Edition, Oxford, 1954.
2. Knopp, K. .. — *Theorie und Anwendung der Unendlichen Reihen*, 4th edition, Springer-Berlin, 1947.
3. Pillai, S. S. and Chowla, S. D. — "On the error terms in some asymptotic formulæ in the theory of numbers—I," *Jour. Lond. Math. Soc.*, 1930, **5**, 95–101.

DECAY OF SAMARIUM-153

By M. C. Joshi, B. N. Subbarao and B. V. Thosar
(*Tata Institute of Fundamental Research, Bombay*)

Received April 1, 1957
(Communicated by Prof. B. Peters, F.A.SC.)

Abstract

Radiations emitted in the decay of Samarium-153 have been studied in the Siegbahn-Slätis *beta*-ray spectrometer. Using the internal conversion electron spectrum and the photo-electron spectrum with tin as radiator, the internal conversion coefficient α_k has been determined for 102 Kev. and 70 Kev. *gamma*-rays. The relative intensities of the three *beta*-ray branches have been determined. A weak *gamma*-ray of energy 83 Kev. has been found and can be interpreted as a transition to the ground state from the first rotational level in Europium-153. The multipole order and character of the 102 Kev. transition is discussed.

Introduction

Samarium-153 (half-life 47 hrs.) decays by β^- emission to several levels in Europium-153 and has been studied by various workers.[1–9] There has been, however, considerable disagreement about the internal conversion coefficient α_k[2,4,9,10] for the 102 Kev. *gamma*-ray and some uncertainty about the relative intensities of the various *beta*-ray groups involved in the decay scheme. As a result of experiments on Coulomb excitation, rotational levels at 82 Kev. and 187 Kev. have been established in Europium-153 and it was of some interest to find out whether these levels are also formed in the *beta*-decay of Samarium-153.

Accurate determination of internal conversion coefficients has assumed special importance as recently there has been a suggestion,[12,13] with some experimental evidence[14] in its favour, that in the case of magnetic dipole (M_1) transitions, the coefficient has a smaller value than that predicted theoretically by Rose,[15] on account of the finite size of the nucleus. The 102 Kev. transition in Europium-153 has been considered by previous workers[1,2,4] to be a mixture of M_1 and E_2 types and the coefficient α_k as determined in this work is discussed from this standpoint.

The method of investigation adopted in this work consisted of three main experiments. In the first place, the continuous *beta*-spectrum was recorded and the Fermi-Kurie plot was constructed. Secondly, the internal

conversion electron spectrum was investigated, giving the relative intensities of conversion lines for different transitions, K/L ratio and the Auger lines. Finally, using tin as radiator, the photo-electron spectrum was recorded, giving relative intensities of unconverted part of the transitions and X-rays in Europium, consequent on internal conversion. From these measurements, the conversion coefficient was calculated. This method of using photo-electron spectrum has not been employed by previous workers for this isotope and has the further advantage of detecting *gamma*-rays of weaker intensity and of low energy.

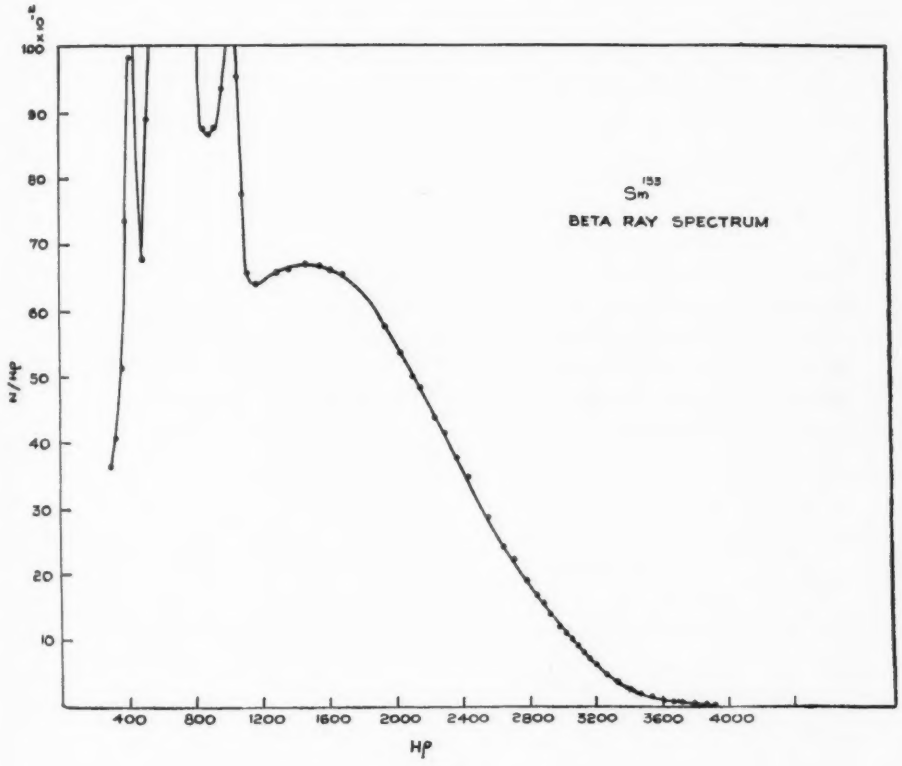

FIG. 1

EXPERIMENTAL OBSERVATIONS AND RESULTS

A source of Samarium-153 of high specific activity was obtained from A.E.R.E., Harwell. Fig. 1 shows the continuous *beta*-ray spectrum of Samarium-153, N/Hρ being plotted against Hρ, the momentum. Fig. 2

is the Fermi plot, the continuous curve having been obtained from the observed points. Assuming allowed shape for different *beta*-groups, this is seen to be made up of three *beta*-ray groups with maximum energies at 792 ± 10 Kev., 685 ± 15 Kev. and 610 ± 20 Kev. respectively. The relative intensities of the *beta*-groups and the Log ft. values for these transitions are given in Table I.

TABLE I

Group	Energy in Kev.	% Transition	log ft.
β_1	792±10	20	7·3
β_2	685±15	65	6·5
β_3	610±20	15	7·1

Fig. 3 shows the internal conversion electron spectrum. The source was deposited on a thin aluminium foil (0·13 mg./cm.^{2}), and was about 100 μg./cm.^{2} in thickness. Five electron peaks are clearly observed and are interpreted as arising from two transitions corresponding to 102 Kev. and 70 Kev. and Europium X-rays, as shown in Table II. Absorption in the counter window, which was 80 μg./cm.^{2} thick, was taken into account, using correction factors obtained from auxiliary experiments using various values for window thickness.

TABLE II

Line energy (Kev.)	Interpretation	Relative intensity	Sum (Kev.)	*Gamma* energy (Kev.)
20·3±·5 ..	K_2 (K conv. of 70 Kev.)	0·29±·03	69·5	70
33±1 ..	A_1 (Auger, K–2L)	$\frac{A_1+A_2}{K_1} = \cdot 19 \pm \cdot 04$		
38±2 ..	A_2 (Auger, K–L–M)			
53·3±1 ..	K_1 (K conv. 102 Kev.)	1	102·5	102
62 ..	L_2 (L conv. 70 Kev.)	0·06±·01	70	70
93·5±3 ..	L_1 (L conv. 102 Kev.)	0·16±·02	101·5	102

Photo-electron spectrum of *gamma*-rays emitted in the decay of Samarium-153 was studied in the present investigation, using different radiators, namely, tin, uranium and gold. Fig. 4 shows the photo-electron spectrum, for tin as radiator. In this experiment, the source was kept close to an aluminium disc, thick enough to absorb all primary *beta*-rays. A layer of tin, 250 μg./cm.^{2} was deposited by evaporation, on one side of the disc, facing

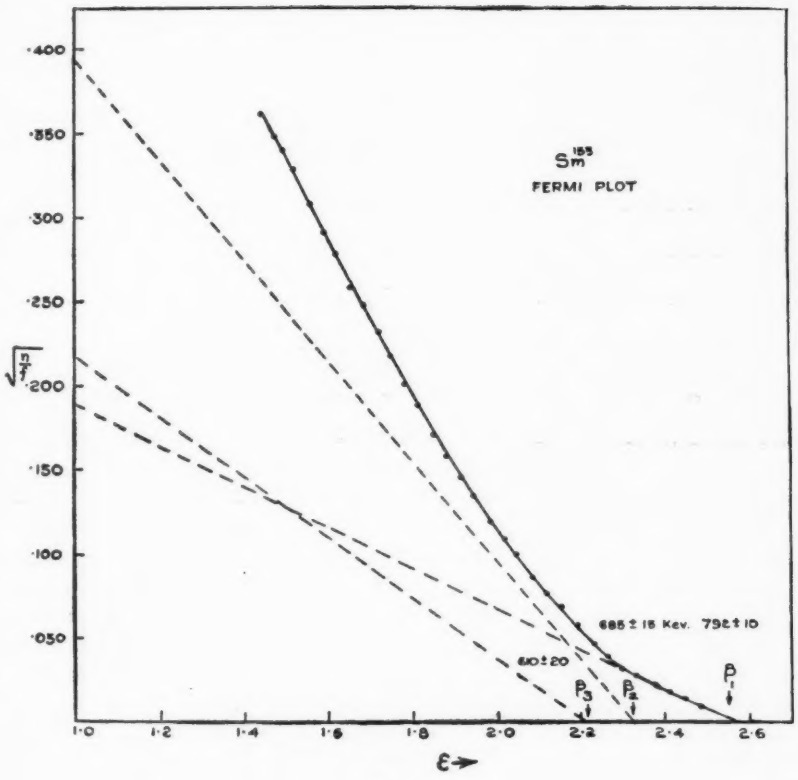

FIG. 2

the spectrometer entrance slit. The line energies measured from the spectrum and their interpretation are shown in Table III. Lines due to *gamma*-rays at 102 Kev. and 83 Kev. are observed, besides the lines due to Europium K_α and K_β X-rays. The line due to 70 Kev. *gamma*-ray, which is highly converted internally, coincides in energy with the L photo-line of K_β X-ray which appears as a weak line on the high energy wing of the

intense L photo-line due to K_α X-ray in Europium. The relative intensities of the 70 Kev. and 83 Kev. *gamma*-rays, in comparison with 102 Kev. *gamma*-ray were found to be $\cdot 06 \pm \cdot 01$ and $< \cdot 04$ respectively, from the photo-electron spectra as well as the scintillation spectrum.

TABLE III

(Radiator: Tin)

Line energy (Kev.)	Interpretation	Sum (Kev.)	Intensity ratio N_z/N_z after necessary corrections
$10 \cdot 5 \pm \cdot 8$ ..	K conv. Eu K X-rays	39·7	$0 \cdot 77 \pm 0 \cdot 05$
$16 \cdot 5 \pm 1$ ..	K conv. Eu K X-rays	45·7	
19 ± 1	Auger line in Tin	K–L–L	
$35 \cdot 5 \pm 1$ ..	L conv. Eu K X-rays	40	
55 ± 2	K conv. 83 Kev. *gamma*	84·2	
$73 \cdot 5 \pm 1$ ..	K conv. 102 Kev. *gamma*	102·5	
97 ± 2	L conv. 102 Kev. *gamma*	101·5	

Fig. 6 shows the decay scheme of Samarium-153. Three *beta*-groups leading respectively to the 170 Kev. 102 Kev and ground states in Europium and the two main *gamma*-transitions at 102 Kev. and 70 Kev. are shown. The weak radiations at 170 Kev. and 530 ± 20 Kev. which have been reported by previous workers[2,4,6] and at 600 Kev.[9] were observed neither in the photo-electron spectrum nor in the internal conversion spectrum clearly and therefore only an upper limit can be put for their intensities as 1%.

However, they were observed in the scintillation spectrometer with relative intensities $< 1\%$ in comparison with 102 Kev. *gamma*-ray. Since Samarium oxide (Sm_2O_3) 'spec-pure' used for neutron irradiation contains normally Europium as a small impurity, there is a need for some further investigation on these weak transitions. However, contribution due to these weak transitions to the X-ray intensity will be negligible on account of their small internal conversion coefficient, and it has been neglected in the present case. The weak *gamma*-ray at 84 Kev. is shown to be due to the de-excitation of the first rotational level above the ground state. Europium

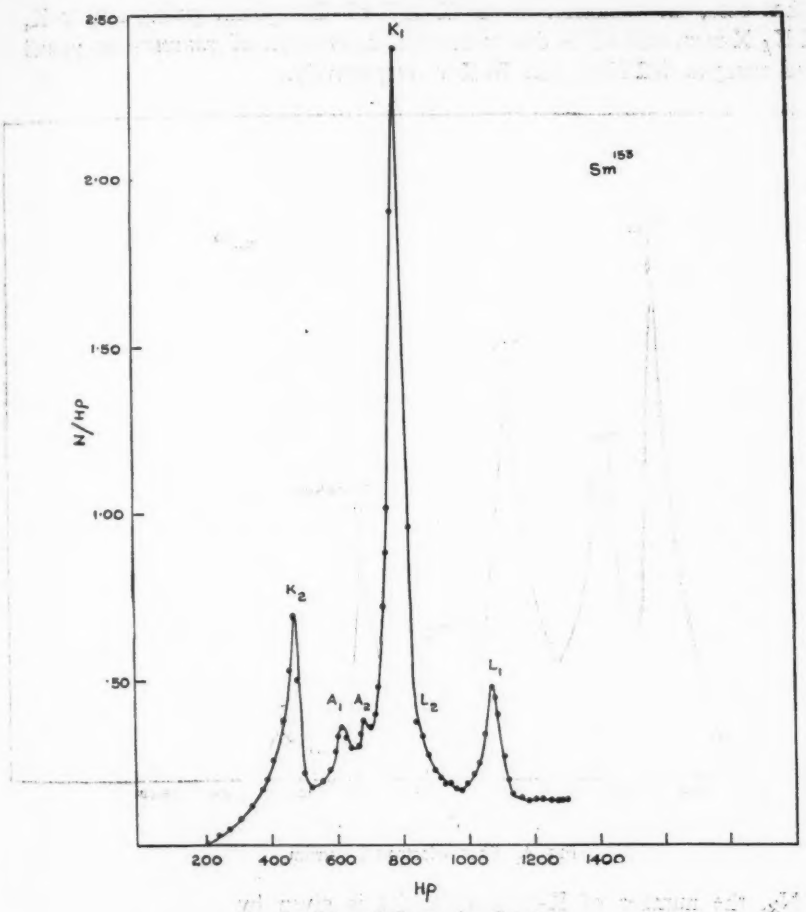

FIG. 3. Internal Conversion Spectrum

155 (half-life 1·7 years) has a *gamma*-ray at 87 Kev. and can be produced as an impurity in the sample but its activity will be less than a thousandth of that of Samarium-153. Also the relative intensities of 83 Kev. and 102 Kev. radiations are seen to remain unchanged over a period of ten days, indicating that 83 Kev. *gamma*-ray observed here is due to Samarium-153. For the purpose of estimating α_K, the conversion coefficient of 102 Kev. *gamma*-ray, and for estimating the relative intensities of the *beta*-branches, the 83 Kev. transition will not be considered. It is also assumed that all the decay is by β^- emission and that there is no decay by electron-capture.

In that case, the vacancies in the K-shell of Europium, giving rise to K_α and K_β X-rays, will all be due to internal conversion of *gamma*-rays γ_1 and γ_2 of energies 102 Kev. and 70 Kev. respectively.

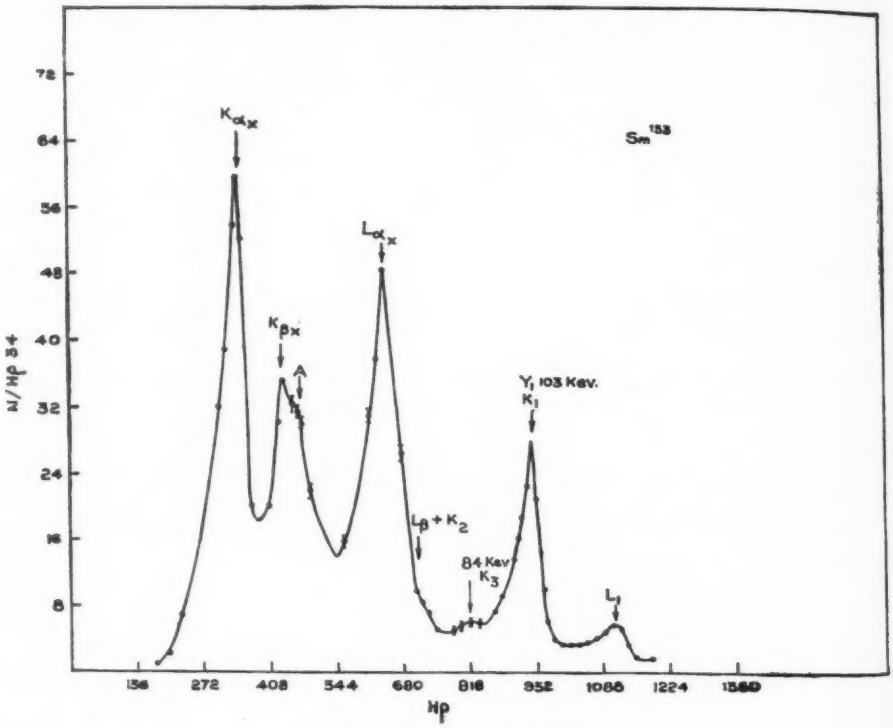

FIG. 4. Photo-electron Spectrum

N_k, the number of K-shell vacancies is given by

$$N_k = N_{ek1} + N_{ek2}$$

where N_{ek_1} and N_{ek_2} represent the number of *gamma*-rays γ_1 and γ_2 converted in the K-shell.

Or,

$$N_k = N_{ek_1}\left(1 + \frac{N_{ek_2}}{N_{ek_1}}\right) \tag{1}$$

Now,

$$N_x = N_k \omega_k \tag{2}$$

where N_x is the number of X-rays and ω_k is the fluorescence yield. Denoting the number of unconverted transitions by N_{γ_1}

$$\frac{N_x}{N_{\gamma_1}} = \frac{N_k \cdot \omega_k}{N_{\gamma_1}}$$

$$\frac{N_x}{N_{\gamma_1}\omega_k} = \frac{N_k}{N_{\gamma_1}} = \frac{N_{ek_1}\left(1 + \frac{N_{ek_2}}{N_{ek_1}}\right)}{N_{\gamma_1}}$$

By definition, α_{k_1}, the internal conversion coefficient of γ_1 is $\frac{N_{ek_1}}{N_{\gamma_1}}$

$$\frac{N_x}{N_{\gamma_1}\omega_k} = \alpha_{k_1}\left(1 + \frac{N_{ek_2}}{N_{ek_1}}\right) \tag{3}$$

The value of α_{k_1} is given by equation (3). The term N_{ek_2}/N_{ek_1} on the right is the ratio of intensities of K-conversion lines due to γ_1 and γ_2 and is obtained from the conversion electron spectrum (Fig. 3) N_x/N_{γ_1}, on the left is the ratio of the intensity of X-rays and of unconverted γ_1-rays and is obtained from the photo-electron spectrum, from the area of the photo-line due to γ_1 and the area under all the photo-lines due to X-rays (Fig. 4), correcting for the variation of photo-electric absorption cross-section in tin with energy. Correction has also to be applied for absorption in the aluminium absorber used for absorbing primary *beta*-rays. One obtains

$$\frac{N_x}{N_{\gamma_1}} = \frac{N_{px}}{N_{p\gamma_1}} \frac{e^{-\mu_{\gamma_1} t}}{e^{-\mu_x t}} \frac{(1 - e^{-\mu\tau_{\gamma_1} l})}{(1 - e^{-\mu\tau_x l})},$$

where N_{px} and $N_{p\gamma_1}$ are the areas under the photo-peaks due to X-rays and γ_1-rays, μ_{γ_1} and μ_x are total absorption coefficients for γ_1-rays and X-rays in aluminium, thickness t (440 mg./cm.^{2}) and $\mu\tau_{\gamma_1}$ and $\mu\tau_x$ are corresponding photo-electric absorption coefficients for tin, thickness, (0·250 mg./cm.^{2}), l, as obtained from the tables.[2]

The fluorescence yield ω_k is obtained from the internal conversion spectrum, from the equation

$$N_k(1 - \omega_k) = N_{Ae}.$$

Where N_k, the number of K-shell vacancies is given by the area under the K-conversion lines of the transitions corresponding to γ_1 and γ_2 and N_{Ae}, the number of Auger electrons, by the area under the Auger lines. The value of ω_k is found to be $0{\cdot}87 \pm {}^{\cdot 04}_{\cdot 02}$, in agreement with $\omega_k = {\cdot}88 \pm {\cdot}02$ given by K. Siegbahn.[2] α_k for 102 Kev. *gamma*-ray as calculated in the above manner is found to be $0{\cdot}69 \pm {\cdot}08$ which agrees with ${\cdot}66 \pm {\cdot}1$ obtained

in the usual manner from the internal conversion line and the β spectrum on which it is superposed. These present values can be compared with $\alpha_k = 0{\cdot}62 \pm {\cdot}15$ given by Lee and Katz[4] and $\alpha_k \sim {\cdot}6$ given by Siegbahn.[3] Now α_k for 70 Kev. transition can be calculated by using the α_k for 102 Kev. transition, the ratio of K internal conversion, *i.e.*, N_{ek_2}/N_{ek_1} and the ratio of *gamma*-ray intensity for these two transitions; α_k for 70 Kev. transition comes out to be $3{\cdot}5 \pm 1{\cdot}4$. This value of α_k for 70 Kev. can be compared with 3·8 given by McGowan,[10] and $4{\cdot}4 \pm {\cdot}4$ given by Dubey *et. al.*[9]

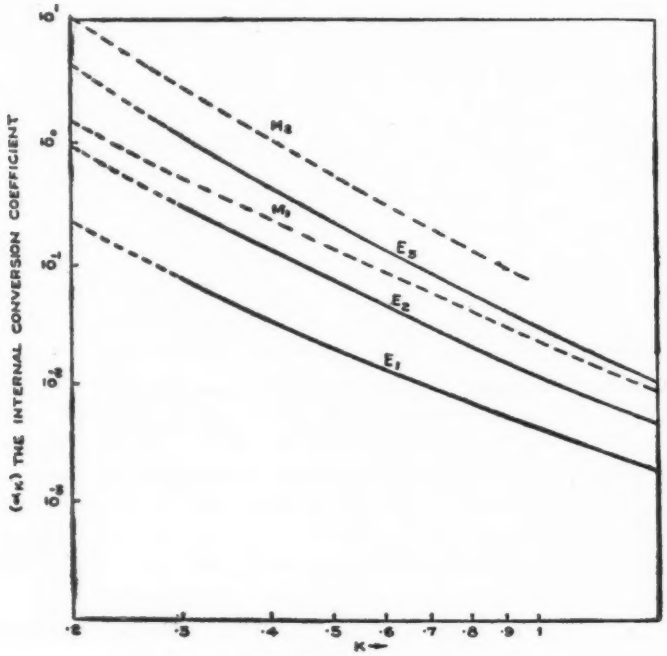

FIG. 5. Photon Energy in Units of mc.²

The branching ratio for the β_1 transition, leading to the ground state in Eu^{153}, is readily found from the Fermi plot (Fig. 2) and is 20%. One can calculate the branching ratio for β_2 and β_3 transitions, making use of the internal conversion data found from the conversion electron spectrum. Referring to the decay scheme and denoting the number of γ_1 and γ_2 transitions by N_1 and N_2 respectively, and the number of the two *beta*-transitions by N_{β_2} and N_{β_3}, one gets,

$$N_{\beta_3} = N_2$$

and

$$N_1 = N_{\beta_2} + N_{\beta_3}$$

$$\therefore \quad \frac{N_1}{N_2} = \frac{N_{\beta_2} + N_{\beta_3}}{N_{\beta_2}} = 1 + \frac{N_{\beta_3}}{N_{\beta_2}}.$$

Also, the number of transitions N_1 equals the number of unconverted γ_1 rays, N_{γ_1}, and the number converted in K and L shells.

$$N_1 = N_{ek_1} + N_{eL_1} + N_{\gamma_1}$$

$$N_1 = N_{ek_1}\left(1 + \frac{N_{eL_1}}{N_{ek_1}} + \frac{N_{\gamma_1}}{N_{ek_1}}\right)$$

$$\therefore \quad N_1 = N_{ek_1}\left(1 + \frac{L_1}{K_1} + \frac{1}{\alpha_{k1}}\right)$$

similarly,

$$N_2 = N_{ek_2}\left(1 + \frac{L_2}{K_2} + \frac{1}{\alpha_{k2}}\right)$$

$$\frac{N_1}{N_2} = \frac{N_{ek_1}}{N_{ek_2}} \frac{\left(1 + \frac{L_1}{K_1} + \frac{1}{\alpha_{k_1}}\right)}{\left(1 + \frac{L_2}{K_2} + \frac{1}{\alpha_{k_2}}\right)}.$$

The quantities on the right, conversion coefficients, K/L ratio and the ratio of intensities of the K-conversion lines for γ_1 and γ_2 are known from the internal conversion spectrum. Hence, N_1/N_2 and N_{β_2}/N_{β_3} can be calculated. The branching ratios for β_2 and β_3 are found to be $N_{\beta 2}/N_{\beta_3} = 5$.

The results are summarised below:

Gamma-ray	α_k	K/L	Intensity
102 Kev.	$0{\cdot}69 \pm 0{\cdot}08$	$6{\cdot}2 \pm {\cdot}8$	1
70 Kev.	$3{\cdot}5 \pm 1{\cdot}4$	$5^{+1{\cdot}3}_{-\ {\cdot}9}$	$0{\cdot}06 \pm 0{\cdot}01$
83 Kev.	..	..	$< {\cdot}04$

$$\beta_1/\beta_2/\beta_3 = 0{\cdot}3/1/0{\cdot}2$$

Discussion of Results

One of the objectives of this work was to determine the K-conversion coefficient for 102 Kev. *gamma*-ray, about which there has been a lack of

agreement among previous workers.[1–9] McGowan[10] and Marty[6] found it to be $1{\cdot}14 \pm {\cdot}2$ and $1{\cdot}2 \pm 0{\cdot}1$ respectively, while Lee and Katz[4] and K. Siegbahn[2] reported it to be of the order of $0{\cdot}6$. The value as determined here is $0{\cdot}69 \pm {\cdot}08$. In the light of this, it is of interest to consider the character and multipole order of the 102 Kev. transition. Previous workers have assumed this transition to be a mixture of E_2 and M_1. Table IV below gives the theoretically expected values for conversion coefficient α_k, and K/L ratio, for this energy and character E_1, E_2, M_1 and M_2. Fig. 5 gives the value of the coefficient α_k for $Z = 64$, against energy in units of $mc.^2$ down to ·3, for E_1, E_2, E_3 and M_1 and M_2 types of transition and the curves as extrapolated to $0{\cdot}2$ corresponding to 102 Kev. These curves are plotted from the tables of conversion coefficient by Rose *et al.*,[15] and the values for α_k in Table IV are obtained from these extrapolated curves.

TABLE IV

E	Z^2/E	α_k				K/L			
		E_1	E_2	M_1	M_2	E_1	E_2	M_1	M_2
102 Kev.	38·53	0·25	0·9	1·5	9·0	6·0	2·0	7·3	5·0

It will be seen from the above consideration that the experimental value for the conversion coefficient for 102 Kev. transition, *i.e.*, $0{\cdot}69 \pm {\cdot}08$ is not in agreement with any one of the theoretical values for the four types of transitions. The value, however, would be consistent with a mixture of E_1 and M_2 types with a preponderant E_1 component.

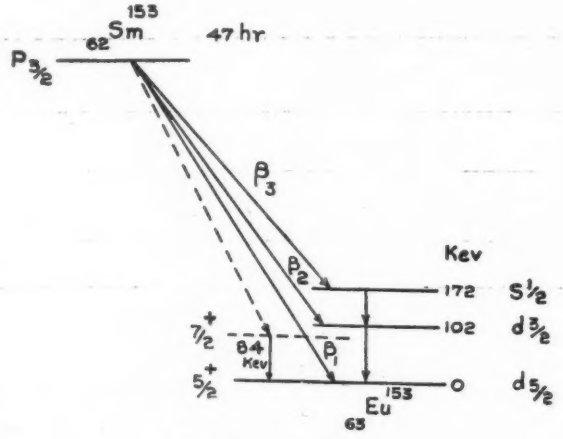

FIG. 6. Decay Scheme

The other alternative is that the transition is a mixture of M_1 and E_2 types, with a correction factor operating in the case of the M_1 coefficient, due to the finite nuclear size, as recently discussed by Sliv[12] and Church.[13] In that case, one finds that it is a predominantly M_1 type of transition and that the correction factor for the coefficient is of the order of 0·5, somewhat larger than that to be expected from Sliv's calculation for nuclei in this range of atomic number.

From shell model considerations the assignment $(d_{5/2}+)$, $(d_{3/2}+)$ and $(s_{1/2}+)$ respectively to the ground, 102 Kev. and 170 Kev. [4,6] states seems resaonable and this would favour the second alternative $(M_1 + E_2)$ for the 102 Kev. transition rather than $(E_1 + M_2)$, as the latter requires a change of parity.

References

1. Rutledge, W. C., Cork, J. M. and Burson, S. B. — *P.R.*, 1952, **86**, 775.
2. Siegbahn, K. .. — *M. Siegbahn Commemorative Volume* (Uppsala), 1951, 237–41.
3. Bannerman, R. C. .. — *Proc. Phys. Soc.*, London, 1952, **65 A**, 565.
4. Lee, M. R. and Katz, R. .. — *P.R.*, 1954, **93**, 155.
5. Hill, J. M. and Snepherd, L. R. — *Proc. Phys. Soc.*, 1950, **63 A**, 126.
6. Marty, N. .. — *J. Phys. Radium*, 1955, **16**, 458.
7. Mihelich, J. W. .. — *P.R.*, 1952, **87**, 646.
8. Graham, R. L. and Walker, J. — *Ibid.*, 1954, **94**, 794.
9. Dubey, V. S. *et al.* .. — *Ibid.*, 1956, **103**, 1430.
10. McGowan, F. K. .. — *Ibid.*, 1954, **93**, 163.
11. Heydenburg, N. P. and Temmer, G. M. — *Ibid.*, 1956, **104**, 981.
12. Sliv, L. A. and Listengarten, M. A. — *Z. Exp. Teor. Fys.* (*U.S.S.R.*), 1952, **22** (1) 9.
13. Church, E. L. and Wesener, I .. — *P.R.*, 1956, **104**, 1382.
14. Nordling, *et al.* .. — *Nuc. Phys.*, 1956, **1**, 326.
15. Rose, M. E., *et al.* .. — *O.R.N.L.*, 1951, 1023.
16. Goldhaber, M. and Sunyar, A. W. — *P.R.*, 1951, **83**, 906.

GENERALISED THEORY OF INTERFERENCE AND ITS APPLICATIONS

Part III. Interference Figures in Transparent Crystals

By S. Pancharatnam

(*Memoir No. 97 from the Raman Research Institute, Bangalore-6*)

Received April 11, 1957

(Communicated by Sir C. V. Raman)

§ 1. Introduction

Among the most beautiful and interesting phenomena in crystal optics are the interference figures displayed by crystalline plates in convergent light. Figures of the most diverse descriptions are met with even in the realm of transparent crystals, and this is not a matter for surprise: for, firstly the crystal may possess optical activity—in which case the two waves propagated along any direction in the medium are in general elliptically polarised; and secondly the state of polarisation of the incident light as well as that of the light for which the analysing arrangement is completely transparent may be adjusted to be linear, circular or elliptic in form. By the use of the Poincaré sphere, the varied phenomena which fall under this head may be brought under a general method of analysis, which—without complicating the explanation of the simpler phenomena—helps in the understanding of more complex phenomena.

As specific applications of the method we shall consider some of the interference figures displayed by the optically active crystal, quartz. Using a single basal section, an interference figure consisting of two spirals coiled around each other may be obtained with a circular polariser and a linear analyser. This case has been theoretically discussed in the treatises of Walker,[1] Pockels[2] and Szivessy[3] (though, due to certain minor errors, the final description of the spirals given in these treatises differ as regards the handedness and orientation of the spirals). When a usual polarising microscope is used, the quarter-wave plate has be to inserted just prior to the analysing nicol, and hence the spirals have to be observed under an arrangement slightly different from that considered in the above-mentioned references. The spirals thus observed with a linear polariser and a 'circular analyser' are discussed in the treatise of Mascart.[4] The sense of description of the spirals is reversed when the quarter-wave plate is transferred from a position behind the quartz plate to a position in front of it (though Mascart states that the same results are obtained under both arrangements).

We shall also discuss from a novel point of view, the *Airy's spirals* observed when two basal sections of quartz of equal thickness and of opposite sign are superposed, and the combination observed between crossed nicols in convergent light.

§ 2. Discussion of the General Case

As is well known, each point in a convergent light figure is the focal point of a particular bundle of *parallel* rays emerging from the plate, of which each pair of rays which have been derived by the splitting of a common incident ray, can (after passing through the analysing arrangement) interfere at the focal point. Hence our first step is to discuss the interference effects presented in *parallel light* at normal incidence by an arbitrarily cut plate of any transparent material when examined between an elliptic polariser C_1 and an elliptic analyser C_2.† The crystal being transparent, the two waves propagated through it must necessarily be in two oppositely polarised states A and A′ as indicated in Fig. 1 (since only then will the intensity of the emerging beam be independant of the phase retardation introduced by the plate [Part I,[5] §2]).

When the incident light (of unit intensity) in the state of polarisation C_1 is split into two beams of opposite polarisation A and A′, these component beams will have the intensities $\cos^2 \frac{1}{2}a_1'$ and $\sin^2 \frac{1}{2}a_1'$ respectively, where a_1' is the angular distance between the states C_1 and A on the Poincaré sphere (Part I, §2). The analyser C_2 transmits the fractions $\cos^2 \frac{1}{2}a_2'$ and $\sin^2 \frac{1}{2}a_2'$ of these beams, since it transmits only the corresponding resolved components[5,6] of these beams in the state of polarisation C_2; here a_2' is the angular separation between the states C_2 and A on the Poincaré sphere. Taking the state of relative phase of the two oppositely polarised beams at the point of entry in the medium as the zero or standard, their phase difference at the point of emergence from the crystal will be equal to δ (which is the path retardation suffered by the slower beam of polarisation A′ relative to the other). The phase difference between the corresponding resolved components transmitted by the analyser will however be smaller than this value by an angle $\hat{A}$; according to Part I, eq. 9, $\hat{A}$ denotes now half the area of the lune $AC_1A'C_2A$, or $\hat{A} = \angle C_2AC_1 = \angle C_1A'C_2$. (The angles are measured with the usual sign convention, being reckoned positive in a counter-clockwise sense [see Fig. 1]).

---

† An elliptic analyser C_2 appears completely transparent for light of *elliptic* polarisation C_2; a quarter-wave plate followed by a linear analyser together form a simple elliptic analyser (Part I §8).

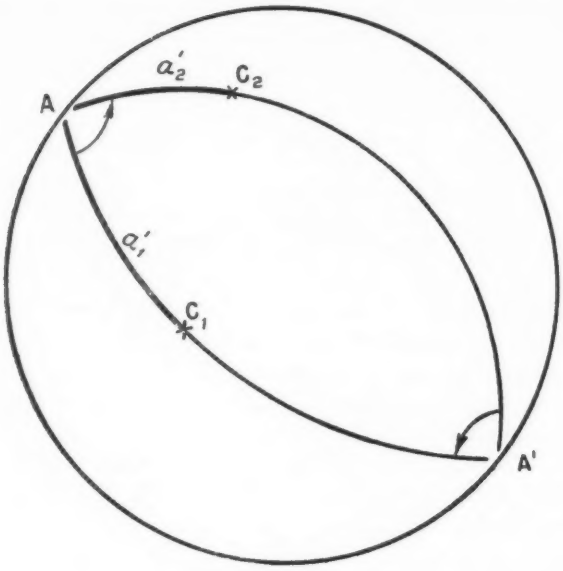

FIG. 1.

Thus the analyser C_2 transmits two beams having intensities I_1 and I_2 and phase difference $\triangle$ given by

$$\left.\begin{aligned} &I_1 = \cos^2 \tfrac{1}{2}a_1' \cos^2 \tfrac{1}{2}a_2'; \quad I_2 = \sin^2 \tfrac{1}{2}a_1' \sin^2 \tfrac{1}{2}a_2' \\ &\triangle = \delta - \hat{A} \end{aligned}\right\} \qquad (1)$$

These beams being in the same state of polarisation, the final intensity I transmitted by the analyser will be given by the usual interference formula

$$I = I_1 + I_2 + 2\sqrt{I_1 I_2} \cos \triangle \qquad (2)$$

The expression for the intensity I can also be written as the difference of two terms, the first of which is the intensity $\cos^2 \frac{1}{2} \widehat{C_1 C_2}$ which would be transmitted if the plate were absent ($\delta = 0$), the second term giving rise to subtraction colours in white light.

Equations (1) and (2) are the basic equations on which the further discussion of all interference phenomena shown by transparent crystals are based. Though they have been derived for the most general case they are practically identical with those customarily used[7] for the simplest case, *viz.*, when the plate possesses only linear birefringence, and the polarising and

analysing elements are nicols—in which case $\hat{A}$ is equal to zero or π. In discussing any specific case, the values of the angles a_1', a_2' and A which obtain in that case have to be used; but their explicit values need be introduced not in the general expression (2), but only in certain subsidiary expressions determining those particular aspects of the phenomena which are to be investigated.

The variation of I with the direction of propagation may be observed in convergent light, using a plate cut normal to an optic axis—each *point* in the convergent light figure corresponding to a definite *direction* of propagation. For a plate of moderate thickness the retardation δ introduced by the plate increases rapidly as we proceed outwards along directions normal to the curves of constant retardation. The rate of variation of I as we proceed outwards from the optic axis is therefore taken to be predominantly due to the change in $\triangle$. We should therefore expect the appearance of interference rings, the curves of minimum intensity occurring along directions for which the pairs of pencils transmitted by the analyser ' destructively ' interfere, *i.e.*, along the curves where $\triangle = (2n + 1)\pi$. These do not however coincide with the curves where the retardation of the plate is an odd multiple of π. The physical reason for this is that the final phase difference $\triangle$ between the interfering pencils transmitted by the analyser is not identical with the retardation introduced by the plate but exceeds it by an amount $(-\hat{A})$; this latter may be correctly described as the contribution to the phase difference arising from the processes of dissolution and analysation, and it depends on the mutual relation between the state of incident polarisation C_1, the states of polarisation A and A′ of the beams into which it is split, and the analysing state C_2. The curves of minimum intensity are thus given by

$$\delta = (2n + 1)\pi + \hat{A} \tag{3}$$

and from what has been said above, *these curves of minimum intensity do not in general follow the curves of constant retardation*, $\delta = \text{const.}$, because the angle A is not constant but is itself a function of the direction of propagation (since the states A and A′ vary with the direction of propagation). A fairly accurate method of plotting the curves of minimum intensity (for a uniaxial crystal or a biaxial crystal of not too small an axial angle) is obviously the following; the circular curve $\delta = (2n + 1)\pi$ is first drawn and the radii vectors of this curve are increased by amounts which vary with the azimuth and which correspond to an additional retardation of $\hat{A}$. In this manner it can be shown that the interference rings exhibited by a basal

section of quartz between inclined nicols take the form of squares with rounded corners.

The intensity at any point on a curve of minimum intensity may be obtained by substituting $\triangle = \pi$ in (2) and is given by

$$I_{min} = \cos^2 \tfrac{1}{2}(a_1' + a_2') \tag{4}$$

This is not constant along a curve of minimum intensity, since the states A and A′ vary with direction, and hence the rings appear darkest along particular zones which have to be determined for each specific case.

§ 3. Spiral Figures Due to a Single Basal Section of Quartz

In discussing the convergent light figures of quartz we will have to keep in mind the following features regarding the propagation of light near the optic axial direction. Referring to Fig. 2 *a*, consider any point P in the convergent light figure, whose polar co-ordinates are r, θ (the origin O representing the optic axial direction, and OV being a vertical line). Along the direction represented by P are propagated two crossed elliptic vibrations; and since quartz is a positive crystal, the major axis of the *slower*

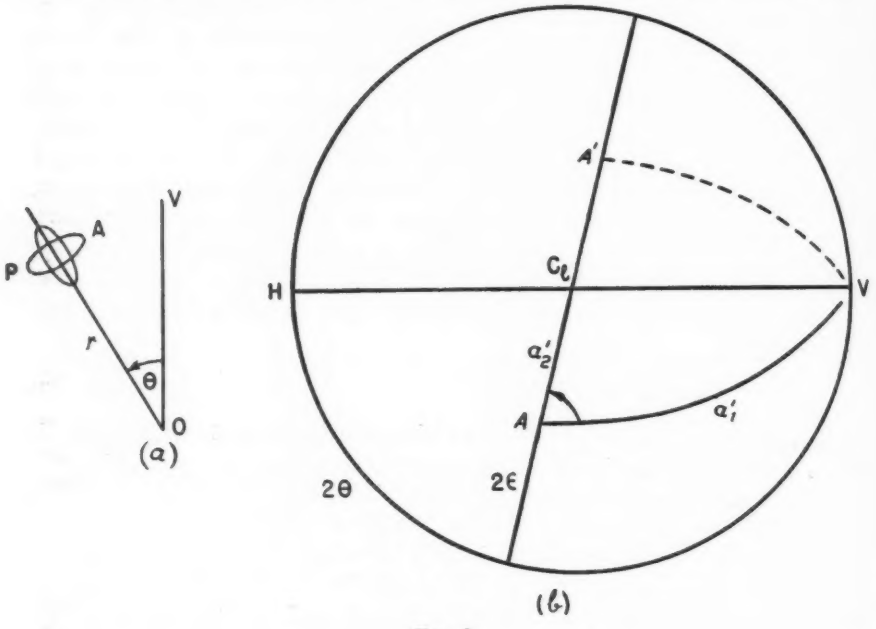

FIG. 2.

vibration coincides with the plane of the radius vector OP itself (so that θ is the azimuth of the major axis of the faster vibration A with respect to the horizontal). Hence if ϵ be the ellipticity of the faster wave, its state of polarisation will be represented on the Poincaré sphere (Fig. 2 *b*), by the point A of longitude 2θ and latitude 2ϵ, ϵ being positive or negative according as the crystal is optically left or right handed. The numerical value of the ellipticity decreases rapidly as the angular distance r from the optic axis increases, ($\tan 2\epsilon = 2\rho/Ar^2$), being a maximum along the optic axial direction where opposite circular vibrations are propagated. In what follows the main fact to remember is that for all points P on a circle of radius r, the ellipticity is constant—so that the latitude 2ϵ of the point A is constant, only the longitude 2θ being altered.

We shall first discuss the interference figure presented by a left-rotating basal section when a left-circular analyser (represented by the pole C_l in Fig. 2 *b*) is used, the vibration direction of the incident *plane* polarised light being vertical (represented by the point V). In this case we have $\hat{A} = \angle C_lAV$. It is seen immediately from Fig. 2 *b* that (keeping 2ϵ constant) as 2θ increases from $0 \rightarrow \frac{1}{2}\pi \rightarrow \pi \rightarrow 3\pi/2 \rightarrow 2\pi$, the $\angle C_lAV$ also increases continuously and goes through the same range of values $0 \rightarrow \frac{1}{2}\pi \rightarrow \pi$; $-\pi \rightarrow -\frac{1}{2}\pi \rightarrow 0$. This means that along the circle $\delta = (2n + 1)\pi$, the phase difference $\triangle$ between the interfering pencils transmitted by the analyser falls short of $(2n + 1)\pi$ (condition for destructive interference) by an angle C_lAV which increases continuously with the azimuth θ — and which in fact becomes exactly equal to *twice* the azimuth at $\theta = m\pi/4$. It follows immediately (see Section 2) that the curves of minimum intensity consist of two mutually enwrapping *left-handed* spirals which are related to one another by a rotation of 180°. From the triangle VAC_l we have

$$\tan \angle C_lAV = \tan 2\theta/\sin 2\epsilon \qquad (5)$$

In the usual treatment[4] equations (3) and (5) are derived by a more lengthy procedure, and these equations may be used to discuss the form of the spirals in more detail. Close to the optic axial direction we have $\angle C_lAV \simeq 2\theta$, so that the spirals are given by:

$$\delta = \sqrt{(Ar^2 + 4\rho^2)} = (2n + 1)\pi + 2\theta$$

If the two arms of the spiral be extrapolated to the origin (where they actually fade away) the common tangent at the origin will be at an azimuth $(\frac{1}{2}\pi + \rho)$ with respect to the vertical—where ρ is the total optical rotation along the optic axis. Towards the border the figure must approximate to the non-spiral form shown by inactive crystals. The transition occurs by

way of the non-uniform rate of increase of the arm of the spiral—which manifests itself as kinks, which in turn assume the proportion of discontinuities towards the border of the figure (see Pockels, Plate VI, Figs. 3 and 4).

The zones along which the successive arcs of the spiral appear darkest may be determined with sufficient accuracy by studying the variation of (4) along a circle described about the optic axis ($a_2' = \text{constant}$). Referring to Fig. 2 *b*, the arc a_1' acquires its maximum value of $(\pi - 2\epsilon)$ at $2\theta = 0$, and its minimum value of 2ϵ at $2\theta = \pi$. Along directions close to the optic axis (where $2\epsilon > \pi/4$) the sum $(a_1' + a_2')$ lies between the limits $\frac{1}{2}\pi$ to π. Hence the arcs of the spiral appear darkest along the vertical radius of the field of view. This result has also been derived in the usual presentation. We must emphasize however, that for a plate of moderate thickness (say 3 mm.) the above result holds only for points on the first convolution of the spiral, since at greater angular distances $2\epsilon < \pi/4$ (see Pockels, Plate VI, Figs. 3 and 4).

When the analysing state C_2 is changed to its opposite state C_2', the result (as is seen from Fig. 1) is to diminish the value of $\hat{A}$ by π and to change the length of the arc a_2' to its supplement. The same alteration in the expression (2) may be produced if the polarising state C_1 is changed to its orthogonal state. Hence, when a right-circular analyser is used, the entire spiral figure is rotated around by a right angle compared to the previous case (when a left-circular analyser was used).

We may obviously summarise the above results in a form applicable to both right and left-rotating basal sections. The handedness of the double spirals exhibited with a linear polariser and circular analyser is always the same as the handedness of the quartz. When the handedness of the circular analyser is opposite to that of the quartz, the tangent to the spiral at the origin coincides with the vibration direction of the light *emerging* along the optic axial direction; and, close to the optic axis, the spirals appear darkest along the diameter perpendicular to the plane of vibration of the incident light. A change in the handedness of the circular analyser causes a rotation of the entire figure, as such, through a right angle.

We see from Fig. 1 that when the state of polarisation of the incident light, and the state of polarisation C_2 of the light for which the analyser is transparent are interchanged, the sign of $\hat{A}$ is reversed, but the remaining factors in (1) remain unchanged. In Fig. 2 *b* the same result is obtained by change of the sign of 2θ. Hence *the entire spiral figure exhibited with a circular polariser and linear analyser is merely the reflection about the plane of vibration of the analyser, of the figure obtained when the polariser and*

analyser are interchanged. This statement holds with regard to all the details of the figure, and hence we need not discuss this case further.

The results of this section were qualitatively verified using a plate of right-quartz. The general arguments may be applied *mutatis mutandis* for discussing the spiral figures in negative uniaxial crystals and in biaxial crystals. In the latter case only a *single* spiral is formed because, as the polar angle of the point P increases, the azimuth of the major axis of the faster elliptic vibration increases at only *half* the rate.

§ 4. Airy's Spirals Due to Two Superposed Basal Sections

Our general treatment can also be applied to the case of superposed transparent plates which often exhibit curious interference figures (see *e.g.*, Walker, *loc. cit.*, p. 293). For this purpose it is necessary to replace the effect of the passage through a succession of plates by a passage through a single 'equivalent plate'. This can be done by combining successive rotations of the Poincaré sphere.

As an example, let us suppose that a left-handed and a right-handed section of quartz (both of the same thickness and cut at the same angle to the optic axis) are superposed (in that order) such that the corresponding principal planes of the two plates are in coincidence, the combination being then viewed in parallel light at normal incidence.

Referring to Fig. 3, let the point A_1 of latitude 2ϵ represent the state of polarisation of the faster elliptic vibration (of ellipticity ϵ) propagated in the first plate; the state of the faster elliptic vibration of ellipticity $(-\epsilon)$ propagated in the second plate is then represented by a point A_2 of the same longitude as A_1, but of latitude (-2ϵ). Let us construct an isosceles triangle $A_1 X A_2$ as indicated, such that the base angles A_2A_1X and XA_2A_1 are both equal to $\delta/2$ where δ is the retardation of each plate.

The action of the first plate is equivalent to an anti-clockwise rotation of the sphere about A_1 through twice the internal angle at A_1, while the action of the second plate is equivalent to an anti-clockwise rotation about A_2 through twice the internal angle at A_2 (see *e.g.*, Part I, § 6). By a well-known theorem for compounding rotations,[8] the two successive rotations are equivalent to a single rotation about the equatorial diameter through X, through twice the external angle at X. We have thus proved that the *combination is equivalent to a single optically inactive birefringent plate* of retardation $\triangle$, the faster vibration direction of which makes an angle $-\alpha$ with the common principal plane of the two quartz plates (which corres-

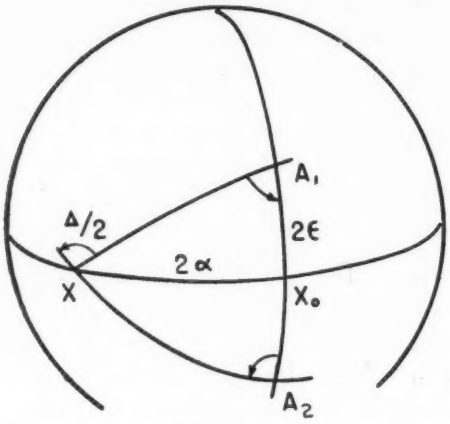

FIG. 3.

ponds to the major axis of the faster ellipse). Here α and $\triangle$ have the values indicated in Fig. 3. From the spherical triangle A_1XX_0 we have

$$\tan 2\alpha = \tan \tfrac{1}{2}\delta \sin 2\epsilon \qquad (6)$$

Since the equivalent plate does not possess optical activity we should expect the appearance of 'isogyres' when two equal basal sections of left- and right-quartz are superposed, and the combination observed between crossed nicols. The 'isogyres' should occur along the directions where the 'equivalent' principal planes of the combination coincide with the vibration directions of the polariser and analyser. Since, as we have seen, the equivalent principal planes for any direction of propagation do not coincide with the principal planes of the individual plates the 'isogyres' will *not* take the form of a uniaxial cross. If θ be the azimuth of a point in the field of view with respect to the plane of the polariser, the dark 'isogyres' obviously occur where θ is equal to α or $(\frac{1}{2}\pi + \alpha)$, where α is given by (6). This equation has been derived by an entirely different method of analysis in the usual presentation (Walker,[1] p. 368, eq. 39). According to this equation it may be shown by following the usual treatment that the dark 'isogyres' take the form of four mutually enwrapping left-handed spirals known as Airy's spirals. Besides these spirals we will have dark curves, where the retardation $\triangle$ of the equivalent plate is a whole multiple of 2π, and from Fig. 3 these occur along the circles $\delta = 2n\pi$.

The sense of description of Airy's spirals is reversed when the right-handed plate is placed first because the sign of α is then changed.

5. Summary

The geometric method of specifying states of polarisation by points on the Poincaré sphere is used for giving a unified and physically intelligible approach to the interference phenomena displayed by crystalline plates in parallel or convergent light—under general conditions when the polarising and analysing states are linear, circular or elliptic in form. Examples discussed are the spiral figures exhibited in convergent light (*a*) by a basal section of quartz between a circular polariser and linear analyser (or *vice-versa*), and (*b*) by two superposed basal sections of left- and right-quartz between crossed nicols. The Airy's spirals observed in the latter case are interpreted as the 'isogyres' of the optically inactive plate to which the combination is equivalent.

6. References

1. Walker .. *Analytical Theory of Light*, Cambridge, 1904, 361 *et seq.*
2. Pockels .. *Lehrbuch der Kristalloptik*, Teubner, 1906, 336 *et seq.*
3. Szivessy .. *Handbuch der Physik*, Springer, 1928, Kap 11, 810 *et seq.*
4. Mascart .. *Traite d'Optique*, 1889, Tome 1, 240; 1891, Tome 2, 301, 317.
5. Pancharatnam .. *Proc. Ind. Acad. Sci.*, 1956, **54 A**, 247.
6. Ramachandran and Ramaseshan *J. Opt. Soc. Am.*, 1952, **42**, 49.
7. Ditchburn .. *Light*, Blackie and Sons, 1952, 385.
8. Ames and Murnaghan .. *Theoretical Mechanics*, Ginn and Co., 1929, 83.

INVESTIGATIONS IN NON-AQUEOUS SOLVENTS

Part II.[1] Solubility and Conductances of Some Rare Earth Metal and Thorium Acetates in Ethylenediamine

By T. Muniyappan and B. Anjaneyalu

(*Chemistry Department, Presidency College, Madras*)

Received April 1, 1957

(Communicated by Dr. T. R. Govindachari, F.A.SC.)

Abstract

In investigations preliminary to the study of the electrolysis of certain rare earth metal and thorium salts in anhydrous basic solvents, it was found that anhydrous acetates of La^{+3}, Ce^{+3} and Th^{+4} are moderately soluble in anhydrous ethylenediamine. The resulting solutions show the conductance behaviour of weak electrolytes. Cerium (III) acetate solution in ethylenediamine undergoes oxidation in air to cerium (IV).

Introduction

The electrodeposition of the rare earth metals and thorium is usually accomplished by the use of their molten halide mixtures; but the possibilities of lower temperature depositions from electrolytic solutions are interesting from the theoretical and practical aspects. Inasmuch as the highly electropositive nature of these metals preclude their electrodeposition from aqueous solutions of its salts owing to the preferential hydrogen discharge, such procedures must of necessity involve basic non-aqueous solvents. Such solvents, because of their strong donor characters, provide media in which solvated electrons can readily exist and in which lower oxidation states are strongly stabilised. The stabilities of alkali and alkaline earth metals in liquid ammonia are well known. The formation of solvolysis products of limited solubility with anhydrous rare earth metal and thorium compounds preclude the use of liquid ammonia. The favourable electrolytic properties of anhydrous ethylenediamine,[2] the success which has been achieved in the electrodeposition of certain alkali[7] and rare earth metals from this medium[3–6] and the failure to electrodeposit thorium from thorium (IV) chloride in this solvent[1] prompted investigation of electrolytic behaviour of anhydrous acetates of some rare earth metals and thorium in anhydrous ethylenediamine. The present investigation reports data on solubilities and conductances of acetates of lanthanum (III), cerium (III) and thorium (IV) in anhydrous ethylenediamine. In a

subsequent communication, results of electrolysis experiments will be described.

Experimental

1. *Purification of solvent.*—Commercial ethylenediamine monohydrate (B.D.H.) was dehydrated and purified as previously outlined.[1] The anhydrous product had a specific conductance of $1 \cdot 35 \times 10^{-6}$ mho cm.$^{-1}$ at 30° C. It was stored in glass-stoppered flasks sealed with Dow-Corning silicone high vacuum grease which has been found to have very little effect on electrical conductance in this solvent. These flasks were kept in desiccators containing soda lime, magnesium perchlorate and phosphorus (V) oxide and were opened only in a dry box since ethylenediamine absorbs both moisture and carbon dioxide from the atmosphere.

2. *Preparation of metal acetates.*—The usual method of obtaining anhydrous metal acetates was by the high temperature reaction of the respective oxides with excess quantities of ammonium acetate, followed by the removal of the unreacted ammonium salt by heating first in a current of dry nitrogen and then *in vacuo*.[9] Anhydrous acetates of lanthanum (III), cerium (III) and thorium (IV) were obtained by the reaction of the respective analytically pure nitrates with acetic anhydride.[8] It is found that this method adopted by Panda and Patnaik[8] is easy and results in purer products than that obtained by Moeller and Zimmermann through the above high temperature reaction.[9] The composition of these anhydrous acetates were established by ignition to oxides in tared platinum crucibles over a Meker burner.

3. *Apparatus and manipulation.*—All anhydrous materials were handled in moisture- and carbon dioxide-free air in a "Gloved Box, Berkeley Type," Model—R1104 supplied by Scientific Service Inc., California. All the solutions were prepared in this dry box and all apparatus containing such solutions was sealed by Dow-Corning silicone high vacuum grease before removal to the atmosphere.

4. *Solubility determinations.*—The respective powdered metal acetate was added in small amounts slowly and with brisk shaking to 20 ml. of anhydrous ethylenediamine in a big test-tube fitted with ground glass stopper until some sizable amount remained undissolved. Portions of this suspension kept in this stoppered test-tube were thermostated for five days at $30 \pm 0 \cdot 05°$ C. with frequent agitation. Then the tubes were centrifuged for twenty minutes and opened inside the dry box. The rare earth and thorium contents of these solutions were determined by precipitating the hydrous hydroxides from measured volumes with excess water and weighing as ignited oxides in a platinum crucible.

5. *Conductance measurements.*—Conductances of the various solutions were obtained after thermostating at $30 \pm 0{\cdot}05°$ C. at definite dilutions as previously outlined,[1] using a Philips Conductivity Bridge, Model GM4249/01, the current switch of the Bridge being set on 1000 cycles per second and a conductance cell fitted with ground glass stopper and bright platinum electrodes. The cell constant was $0{\cdot}2022$ cm.$^{-1}$ The specific conductance of the solvent was subtracted from that of the solution in each case.

RESULTS AND DISCUSSION

Solubility determinations.—Solubility data obtained are summarised in Table I along with the solubility data obtained by Moeller and Zimmermann[9] for purposes of comparative study.

TABLE I

Solubilities of some rare earth metal and thorium salts in ethylenediamine at 30° *C.*

Salt	Solubility in			Ref.
	g./100 ml. of soln.	moles/litre of soln.	g./100 g. of solvent	
La $(C_2H_3O_2)_3$ ..	6·97	0·22	8·01	..
La $(NO_3)_3$ ..	..	..	2·45	9
Ce $(C_2H_3O_2)_3$ ..	10·64	0·34	12·41	..
Nd Br_3 ..	..	..	0·94	9
Nd I_3 ..	..	..	2·53	9
Nd $(C_2H_3O_2)_3$ ..	7·81	0·30	..	9
Y $(C_2H_3O_2)_3$ ..	6·26	0·30	..	9
Th $(C_2H_3O_2)_4$ ..	3·73	0·08	4·30	..
Th Cl_4 ..	11·08	0·30	..	1
Hg $(C_2H_3O_2)_2$ ..	..	..	0·19	11

Anhydrous lanthanum (III) acetate and thorium (IV) acetate gave colourless solutions in ethylenediamine while the solution of cerium (III) acetate was deep brown. That this discolouration was due to atmospheric oxidation of

some part of cerium (III) to cerium (IV) was revealed during the dilution of this solution with water when an immediate violetish blue precipitate of hydrous hydroxide of cerium (III) and cerium (IV) was obtained. Similar atmospheric oxidation of cobalt (II) salts to cobalt (III) salts in ammoniacal solution is common in co-ordination chemistry. The moderately high solubilities of these anhydrous acetates are probably due to the relatively higher covalent nature when compared with the corresponding anhydrous metal halides and nitrates as apparent from Table I. The enhanced solubility of thorium (IV) chloride may be the result of extensive solvation.[1] Of the anhydrous rare earth metal acetates so far investigated, cerium (III) acetate has the highest solubility in anhydrous ethylenediamine.

Conductance studies.—Typical conductance data (equivalent conductance, Λ mhos cm.^{2} equiv.$^{-1}$ and concentration of the salt in gram equivalents per litre, C) as summarised in Table II and Fig. 1, indicate that the anhydrous acetates of lanthanum (III), cerium (III) and thorium (IV) behave as weak electrolytes in anhydrous ethylenediamine.

TABLE II

Conductance data for ethylenediamine solutions at 30° *C.*

Lanthanum (III) acetate			Cerium (III) acetate			Thorium (IV) acetate		
Concn., C, equi./litre	$\sqrt{C}\times10^3$	λ	Concn., C, equi./litre	$\sqrt{C}\times10^3$	λ	Concn., C, equi./litre	$\sqrt{C}\times10^3$	λ
0·3308	575	2·614	1·0060	1003	1·816	0·1040	323	1·215
0·1654	407	2·896	0·5030	709	1·886	0·0520	228	1·435
0·0827	288	3·306	0·2520	502	1·978	0·0260	161	1·814
0·0414	203	3·941	0·1260	355	2·271	0·0130	114	2·312
0·0207	144	4·720	0·0630	251	2·594	0·0065	81	3·076
0·0104	102	5·526	0·0315	178	3·156	0·0033	57	3·748
0·0052	72	6·668	0·0158	126	3·917	0·0016	40	4·791
0·0026	51	8·021	0·0079	89	4·974	0·0008	29	6·073
0·0013	36	9·883	0·0039	63	5·962	0·0004	20	9·414
0·0007	26	11·240	0·0020	43	8·078	..	..	..

Among the three salts investigated, the strength of the electrolyte in ethylenediamine increases in the following order;—thorium (IV) acetate, cerium (III) acetate and lanthanum (III) acetate. The observed order

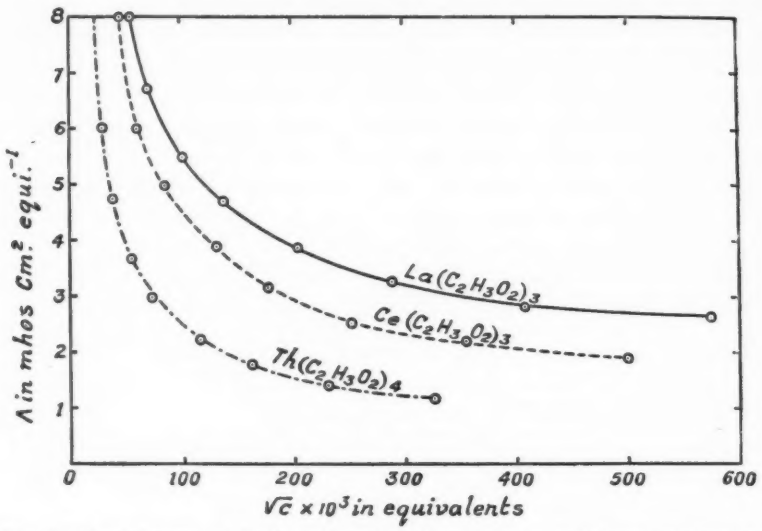

FIG. 1. Conductances of La^{+3}, Ce^{+3} and Th^{+4} acetates in anhydrous ethylenediamine at 30° C.

of increase in equivalent conductance parallels the increase of their ionic radii (Th^{+4} — 1·10; Ce^{+3} — 1·18; La^{+3} — 1·22° A) with the consequent increase in their ionic nature. A comparison of conductance of anhydrous thorium (IV) chloride[1] and anhydrous thorium (IV) acetate shows that the former is a slightly stronger electrolyte in ethylenediamine than the latter since the latter salt is obviously more covalent than the former. The conductance behaviour of other anhydrous salts of the trivalent rare earth metals[3,5,6,9] and a number of other salts[10] indicates that they behave as weak electrolytes in ethylenediamine. This is not surprising when one remembers that compounds containing highly charged cations dissolved in a solvent of only moderately large dielectric constant (ethylenediamine at 25° C. is 12·8) behave as weak electrolytes.

ACKNOWLEDGEMENT

We express our gratitude to Mr. T. Balakrishna Nayar, Principal, Presidency College, Madras, for the award of the College research studentship to the junior author (B. A.) during the progress of this work.

REFERENCES

1. For Part I, see T. Moeller and T. Muniyappan, *J. Nuclear and Inorganic Chemistry* (under publication).

2. Putnam, G. L. and Kobe, K. A. — *Trans. Electro. Chem. Soc.*, 1938, **74**, 609.
3. Zimmermann, P. A. .. *Doctoral Dissertation*, University of Illinois, 1951.
4. Moeller, T. and Zimmermann, P. A. — *Science*, 1954, **120**, 539.
5. Aftandilian, V. D. .. *Doctoral Dissertation*, University of Illinois, 1954.
6. Cullen, G. W. .. *Ibid.*, 1956.
7. Dirske, T. P. and Briscoe, H. T. — *Meta Industries*, 1938, **36**, 284.
8. Patnaik, D. and Panda, S. — *J. Ind. Chem. Soc.*, 1956, **12**, 877.
9. Moeller, T. and Zimmermann, P. A. — *J. Am. Chem. Soc.*, 1953, **75**, 3940.
10. Peacock, J., Schmidt, F. C., Davis, R. E. and Schaap, W. B. — *Ibid.*, 1955, **77**, 5829.
11. Isbin, H. and Kobe, K. A. — *Ibid.*, 1945, **67**, 464.

ADDITION OF AXIALLY SYMMETRIC MOTIONS OF VISCOUS LIQUIDS

By S. K. Lakshmana Rao

Received April 17, 1957
(Communicated by Dr. P. L. Bhatnagar, F.A.SC.)

§ 0. Introduction

The equations of motion of a viscous liquid, *viz.*,

$$\frac{\delta \vec{q}}{\delta t} - \vec{q} \times \operatorname{curl} \vec{q} + \tfrac{1}{2} \operatorname{grad} q^2 = - \operatorname{grad} \left(\frac{p}{\rho} + \Omega \right) + \nu \Delta \vec{q} \quad (0.1)$$

involve non-linear terms and several devices (inverse or semi-inverse methods) have been introduced for studying the equations (0.1). The notion of additivity or superposability of two motions is one such device that has received considerable attention in recent years. If $(\vec{q}_1, p_1, \Omega_1)$ are the flow velocity, the mean pressure and the external force potential of a viscous liquid motion and $(\vec{q}_2, p_2, \Omega_2)$ are the similar quantities for another motion of the liquid, the two motions are additive resulting in the motion $(\vec{q}_1 + \vec{q}_2, p_1 + p_2 + \pi, \Omega_1, + \Omega_2)$ if and only if[1,2]

$$\operatorname{curl} (\vec{q}_1 \times \operatorname{curl} \vec{q}_2 + \vec{q}_2 \times \operatorname{curl} \vec{q}_1) = 0. \quad (0.2)$$

The adjusted pressure π is determined from the equation

$$\vec{q}_1 \times \operatorname{curl} \vec{q}_2 + \vec{q}_2 + \operatorname{curl} \vec{q}_1 = \operatorname{grad} \left(\frac{\pi}{\rho} + \vec{q}_1 \cdot \vec{q}_2 \right). \quad (0.3)$$

The addition of plane motions of viscous liquids has been examined in detail by Ram Ballabh[3] and the problem for axially symmetric motions with the flow velocity vector in the meridian plane has been studied by P. L. Bhatnagar and P. D. Verma.[2*] In the present paper we examine the problem of addition of axially symmetric motions for which the flow velocity vector does not necessarily lie in the meridian plane, so that the velocity $\vec{q}$ can be represented in the form

$$\vec{q} = q_x \vec{i}_x + q_{\widetilde{\omega}} \vec{i}_{\widetilde{\omega}} + q_\omega \vec{i}_\omega \quad (0.4)$$

---

* I am grateful to Prof. P. L. Bhatnagar for bringing this to my notice.

in the notation of L. M. Milne-Thomson.[4] The axial symmetry of the motion requires that q_x, $q_{\tilde{\omega}}$, q_ω depend only on the co-ordinates x and $\tilde{\omega}$ besides the time t. We characterize all such steady motions which are self-additive (Theorem 2 below) and see that the flow velocity can be explicitly represented in a special type of such flows.

REMARK 1. The class of (axially symmetric) motions with the streamlines coincident with the vortex lines is included as a special case of the class of (axially symmetric) self-additive motions.

REMARK 2. The condition for a steady motion of a viscous liquid to have the circulation-preserving property is the same as that for the motion to be self-additive. The results of § 2 below thus also characterize the class of all axially symmetric, steady, viscous liquid flows, which are circulation-preserving.

§ 1. Conditions for addition of motions in the case of axial symmetry.

If

$$\vec{q} = q_x \vec{i}_x + q_{\tilde{\omega}} \vec{i}_{\tilde{\omega}} + q_\omega \vec{i}_\omega$$

is the velocity vector of a motion, the continuity equation, *viz.*, $\operatorname{div} \vec{q} = 0$ is satisfied on writing

$$q_x = -\frac{1}{\tilde{\omega}} \frac{\delta \psi}{\delta \tilde{\omega}}, \quad q_{\tilde{\omega}} = \frac{1}{\tilde{\omega}} \frac{\delta \psi}{\delta x}$$

and we may write $q_\omega = \chi$.

Taking the two motions given by

$$\vec{q}_r = \left(-\frac{1}{\tilde{\omega}} \frac{\delta \psi_r}{\delta \tilde{\omega}}\right) \vec{i}_x + \left(\frac{1}{\tilde{\omega}} \frac{\delta \psi_r}{\delta x}\right) \vec{i}_{\tilde{\omega}} + \chi_r \vec{i}_\omega, \quad (r = 1, 2) \quad (1.1)$$

we obtain from condition (0.3) that

$$\frac{1}{\tilde{\omega}^2} \left[\frac{\delta \psi_1}{\delta x} (\mathrm{E}^2 \psi_2) + \frac{\delta \chi_2}{\delta x} (\mathrm{E}^2 \psi_1) + \frac{\delta}{\delta x} (\tilde{\omega}^2 \chi_1 \chi_2) \right] \vec{i}_x$$

$$+ \frac{1}{\tilde{\omega}^2} \left[\frac{\delta \psi_1}{\delta \tilde{\omega}} (\mathrm{E}^2 \psi_2) + \frac{\delta \psi_2}{\delta \tilde{\omega}} (\mathrm{E}^2 \psi_1) + \frac{\delta}{\delta \tilde{\omega}} (\tilde{\omega}^2 \chi_1 \chi_2) \right] \vec{i}_{\tilde{\omega}}$$

$$+ \frac{1}{\tilde{\omega}^2} \left[\frac{\delta \psi_1}{\delta \tilde{\omega}} \frac{\delta}{\delta x} (\tilde{\omega} \chi_2) + \frac{\delta \psi_2}{\delta \tilde{\omega}} \frac{\delta}{\delta x} (\tilde{\omega} \chi_1) - \frac{\delta \psi_1}{\delta x} \frac{\delta}{\delta \tilde{\omega}} (\tilde{\omega} \chi_2) \right.$$

$$- \frac{\delta\psi_2}{\delta x} \frac{\delta}{\delta\varpi} (\varpi \chi_1)\Big] \vec{i}_\omega$$

$$= \text{grad} \left(\frac{\pi}{\rho} + \vec{q}_1 \cdot \vec{q}_2 \right) \tag{1.2}$$

where E^2 is the differential operation

$$\frac{\delta^2}{\delta x^2} + \frac{\delta^2}{\delta \varpi^2} - \frac{1}{\varpi} \frac{\delta}{\delta \varpi}.$$

Writing $\pi/\rho + \vec{q}_1 \cdot \vec{q}_2 = F$, we have the right-hand side of (1.2) in the form

$$\frac{\delta F}{\delta x} \vec{i}_x + \frac{\delta F}{\delta \varpi} \vec{i}_\varpi + \frac{1}{\varpi} \frac{\delta F}{\delta \omega} \vec{i}_\omega. \tag{1.3}$$

Since $\vec{q}_1$, $\vec{q}_2$ are axially symmetric fields and π also is to be axially symmetric, we have $\delta F/\delta\omega = 0$. In view of this, we get from (1.2), (1.3)

$$\frac{1}{\varpi^2} \left[\frac{\delta\psi_1}{\delta x} (E^2\psi_2) + \frac{\delta\psi_2}{\delta x} (E^2\psi_1) + \frac{\delta}{\delta x} (\varpi^2 \chi_1 \chi_2) \right] dx$$

$$+ \frac{1}{\varpi^2} \left[\frac{\delta\psi_1}{\delta \varpi} (E^2\psi_2) + \frac{\delta\psi_2}{\delta \varpi} (E^2\psi_1) + \frac{\delta}{\delta \varpi} (\varpi^2 \chi_1 \chi_2) \right] d\varpi$$

$$= \frac{\delta F}{\delta x} dx + \frac{\delta F}{\delta \varpi} d\varpi = dF - \frac{\partial F}{\partial t} dt \tag{1.4}$$

and

$$\frac{\delta(\psi_1, \varpi \chi_2)}{\delta(x, \varpi)} + \frac{\delta(\psi_2, \varpi \chi_1)}{\delta(x, \varpi)} = 0. \tag{1.5}$$

By means of cross-differentiation with respect to x, we may derive from (1.4), the single equation

$$\frac{\delta(\psi_1, E^2\psi_2)}{\delta(x, \varpi)} + \frac{\delta(\psi_2, E^2\psi_1)}{\delta(x, \varpi)}$$

$$- \frac{2}{\varpi} \left[\frac{\delta\psi_1}{\delta x} (E^2\psi_2) + \frac{\delta\psi_2}{\delta x} (E^2\psi_2) + \frac{\delta}{\delta x} (\varpi^2 \chi_1 \chi_2) \right] = 0 \tag{1.6}$$

The equation (1.4) can also be written in the form

$$d\left(\frac{\pi}{\rho}\right) = \frac{1}{\varpi^2} [(E^2\psi_1)\, d\psi_2 + (E^2\psi_2)\, d\psi_1] + \frac{1}{\varpi^2}\, d(\varpi^2 \chi_1 \chi_2)$$

$$- d\left[\frac{1}{\varpi^2} \left(\frac{\delta\psi_1}{\delta x} \frac{\delta\psi_2}{\delta x} + \frac{\delta\psi_1}{\delta \omega} \frac{\delta\psi_2}{\delta \omega} \right) \right] \tag{1.4a}$$

and determines the adjusted pressure π.

The above results can be stated as

THEOREM 1. The necessary and sufficient conditions that two axially symmetric flows of a viscous liquid corresponding to $(\psi_a, \chi_a, p_a, \Omega_a)$ $(a = 1, 2)$ may be additive are given by the equations (1·5), (1·6) above. Equation (1·4 *a*) may be used for determining the adjusted pressure π.

§ 2. Self-additive motions.

From the above considerations it follows that the flow given by (ψ, χ, p, Ω) is self-additive, *i.e.*, can be added to itself, if and only if,

$$\frac{\delta(\psi, \varpi\chi)}{\delta(x, \varpi)} = 0 \tag{2·1}$$

and

$$\frac{\delta(\psi, \mathrm{E}^2\psi)}{\delta(x,\varpi)} - \frac{2}{\varpi}\frac{\delta\psi}{\delta x}\mathrm{E}^2\psi - \varpi\frac{\delta}{\delta x}(\chi^2) = 0 \tag{2·2}$$

The equation for determining the adjusted pressure π is easily obtained from (1·4 *a*) in the form

$$d\left(\frac{\pi}{\rho}\right) = \frac{2}{\varpi^2}(\mathrm{E}^2\psi)\,d\psi + \frac{1}{\varpi^2}d(\varpi^2\chi^2) - d\left[\frac{1}{\varpi^2}\left\{\left(\frac{\delta\psi}{\delta x}\right)^2 + \left(\frac{\delta\psi}{\delta\varpi}\right)^2\right\}\right]. \tag{2·3}$$

From (1·4) we have in the case of self-additive motions, also

$$\frac{\delta(\mathrm{F}, \psi)}{\delta(x, \varpi)} = 0 \tag{2·4}$$

where

$$\mathrm{F} = \frac{\pi}{\rho} + q^2,$$

showing that

$$\tfrac{1}{2}\left(\frac{\pi}{\rho} + q^2\right) = g(\psi) \tag{2·5}$$

The equations (2·1) and (2·2) are effectively the same as those obtained by S. Chandrasekhar and Kevin H. Prendergast.[5]

From (2·1) we get

$$\varpi\chi = f(\psi) \tag{2·6}$$

and on using (2·5) and (2·6) in the equation (2·3) we obtain

$$\frac{1}{\varpi^2} E^2\psi + \frac{1}{\varpi^2} f(\psi) f'(\psi) = g'(\psi) \tag{2.7}$$

THEOREM 2. The class of axially symmetric steady flows with the velocity vector

$$-\frac{1}{\varpi}\frac{\delta\psi}{\delta\varpi}\vec{i}_x + \frac{1}{\varpi}\frac{\delta\psi}{\delta x}\vec{i}_\varpi + \chi\vec{i}_\omega$$

is characterized by the conditions (2·6) and (2·7).

In the case of Beltrami flows with the streamlines coincident with the vortex lines, we have $F = a$ constant and $g(\psi)$ of (2·5) becomes a constant.

COROLLARY: The class of axially symmetric, steady, Beltrami flows is characterized by the condition

$$E^2\psi + f(\psi) f'(\psi) = 0 \tag{2.8}$$

The equation (2·8) has been completely integrated by S. Chandrasekhar[6] in the case where $f(\psi) = a$ linear function $= \alpha\psi$. (An additive constant β has no physical consequence.) He has shown that the general solution $\psi(x, \varpi)$ of

$$\left(\frac{\delta^2}{\delta x^2} + \frac{\delta^2}{\delta\varpi^2} - \frac{1}{\varpi}\frac{\delta}{\delta\varpi} + \alpha^2\right)\psi = 0 \tag{2.8 a}$$

can be expressed in terms of the fundamental solutions

$$\phi_n = [A_n J_{n+3/2}(\alpha r) + B_n J_{-(n+3/2)}(\alpha r)]\, r^{-3/2} P_n^{(3/2)}(\cos\theta)$$
$$n = 1, 2, 3, \ldots\ldots \tag{2.9}$$

where $r\cos\theta = x$ and $r\sin\theta = \varpi$, A_n, B_n are arbitrary constants and $P_n^{3/2}(\cos\theta)$ denotes the ultraspherical polynomial.[7] The velocity in such a case [$f(\psi) = a$ linear function] of axially symmetric Beltrami flows can therefore be represented as any linear combination of the vectors

$$\left(-\frac{1}{r}\frac{\delta\phi_n}{\delta r} + \frac{\cot\theta}{r^2}\frac{\delta\phi_n}{\delta\theta}\right)\vec{i}_x$$
$$+\left(\frac{\cot\theta}{r}\frac{\delta\phi_n}{\delta r} - \frac{1}{r^2}\frac{\delta\phi_n}{\delta\theta}\right)\vec{i}_\varpi + \left(\frac{\alpha\phi_n}{r\sin\theta}\right)\vec{i}_\omega$$
$$(n = 1, 2, 3, \ldots\ldots) \tag{2.10}$$

It was shown by P. L. Bhatnagar* that the equation (2·7) can be integrated on taking $g'(\psi) = a$ constant $= \beta$, in addition to $f'(\psi) = a$. Then (2·7) becomes

$$\left(\frac{\delta^2}{\delta x^2} + \frac{\delta^2}{\delta \varpi^2} - \frac{1}{\varpi}\frac{\delta}{\delta \varpi} + a^2\right)\psi = \beta \varpi^2 \tag{2·11}$$

and the solution of this equation is

$$\psi = \frac{\beta}{a^2}\varpi^2 + \text{solution of (2·8 } a\text{)}.$$

The velocity of the flow is given in this case by adding the vector

$$-\frac{2\beta}{a^2}\vec{i}_x + \frac{\beta}{a} r \sin\theta \, \vec{i}_{\varpi} \tag{2·12}$$

to any linear combination of the vectors (2.10).

Summary

Conditions are noted for the addition of two axially symmetric motions of viscous liquids in which the velocities have toroidal as well as poloidal components and characterization relations are obtained for the class of self-additive axially symmetric motions.

References

1. Strang, J. A. .. "Superposable fluid motions," *Communications Fac. Sci. Univ. Ankara*, 1948, **1**, 1–32 (*vide Mathematical Reviews*, 1950, **11**, 472).
2. Bhatnagar, P. L. and Verma, P. D. "On superposable flows" (in the course of publication).
3. Ram Ballabh .. "Two dimensional superposable motions," *J. Ind. Math. Soc.*, 1952, **16**, 191–97.
4. Milne-Thomson, L. M. .. *Theoretical Hydrodynamics* (3rd Edition), 1955, pp. 57–64.
5. Chandrasekhar, S. and Kevin H. Prendergast "The equilibrium of magnetic stars," *Proc. Nat. Acad. Sci. U.S.A.*, 1956, **42**, 5–9.
6. Chandrasekhar, S. .. "On force-free magnetic fields," *Ibid.*, pp. 1–5.
7. Szegö, G. .. *Orthogonal Polynomials*, 1939.

* I am deeply grateful to Prof. P. L. Bhatnagar for this help.

627–57. Printed at The Bangalore Press, Bangalore City, by C. Vasudeva Rao, Superintendent, and Published by The Indian Academy of Sciences, Bangalore.

ERRATUM

Vol. XLV, No. 5, May 1957

Page 298, line 3rd from bottom, *Change* 'high' *into* 'low'.

Supplement to the

"Proceedings of the Indian Academy of Sciences"

INDEX TO VOL. XLV—(A)

AUTHORS' INDEX

Agarwal, J. K. P. .. *See* Ramaiah and others.

Agarwal, S. K. D. .. *See* Saraswat and Agarwal.

See Ramaiah and others.

Ahluwalia, V. K., Mehta, A. C. and Seshadri, T. R. — Constitution of Dalbergin, III, 15.

Anjaneyulu, B. .. *See* Muniyappan and Anjaneyulu.

Bakhru, K. .. *See* Basu and Bakhru.

Balachandran, V. K. .. On certain BS-representations and a characterization of complete Boolean algebras, 35.

Basu, B. K. and Bakhru, K. — The input and output system of the T.I.F.R. computer, 231.

Bhatki, K. S. and Radhakrishna, P. — Carrier-free separation of Sn^{113} from indium, 30.

Bhatnagar, P. L. and Rao, S. K. Lakshmana — Problems on the motion of non-Newtonian viscous liquids—general considerations, 161.

Bhatnagar, P. L. and Verma, P. D. — On superposable flows, 281.

Bhattacharya, P. B. .. *See* Khanna and others.

Chandrasekhar, S. .. The optical rotatory dispersion of quartz, 147.

Dadape, V. V. .. *See* Krishnaprasad and Dadape.

Deniz, V. C., Iyengar, S. B. D. and Ramanna, R. — On a time of flight method of studying the velocity distribution of neutrons from diffusing media, 205.

Farooqui, M. M., Srivastava, S. P. and Neogi, R. N. — A two dimensional ferrite-core memory, 240.

Gupta, K. K. .. Non-relativistic approximation of Bhabha's equation, 336.

Iyengar, S. B. D. .. *See* Deniz, and others.

Iyengar, S. B. D., Mani, G. S., Ramanna, R. and Umakanth, N.	Slowing down and diffusion of neutrons in beryllium oxide, 215.
	Temperature dependence of the slowing down and diffusion constants of neutrons in beryllium oxide, 224.
Jayaraman, A. ..	Optical properties and unit cell parameters of nickel nitrate hexahydrate, 263.
Joshi, M. C., Subbarao, B. N. and Thosar, B. V.	Decay of samarium –153, 390.
Kapur, J. N. ..	Uniqueness of maximum pressure for the cubic form-function in the general theory of composite charges, 177.
Khan, N. A. ..	The characteristic roots of the product of matrices, 84.
Khanna, K. L., Bhatta-charya, P. B. and Prasad, K.	Improvements in colorimetric determinations, III, 89.
Khubchandani, P. G. ..	*See* Shankar and others.
Krishnamoorthy, P. N.	Inhioition of shrinkage in nuclear emulsions, 327.
Krishnaprasad, N. S. and Dadape, V. V.	Preparation of pure U_3O_8 from crude sodium diuranate by intermediate complex formation, 20.
Mani, G. S. ..	*See* Iyengar and others.
Mehta, A. C. ..	*See* Ahluwalia and others.
Muniyappan, T. and Anjaneyulu, B.	Investigations in non-aqueous solvents, II, 412.
Navalkar, M. P. ..	*See* Ramanna and Navalkar.
Neogi, R. N. ..	*See* Farooqui and others.
Nerurkar, N. W. ..	An interpretation of the solar anisotropy of primary cosmic radiation, 341.
Padmanabhan, V. M. ..	*See* Shankar and others.
Pancharatnam, S. ..	Generalised theory of interference and its applications, III, 402.
Parameswaran, M. R. ..	Some applications of Banach functional methods to summability, 377.
Prasad, K. ..	*See* Khanna and others.

Puranik, P. G. and Rao, A. M. Jaya	Raman effect in mixtures of pyridine with phenol, methanol and water (N - - - H hydrogen bond formation), 51.
Radhakrishna, P. ..	*See* Bhatki and Radhakrishna.
Ramachandran, G. N. and Santhanam, M. S.	Structure of elastin, 124.
Ramachandran, G. N.	*See* Sasisekharan and Ramachandran.
Ramaiah, N. A., Agarwal, S. K. D. and Agarwal, J. K. P.	Chromatographic studies on the kinetics of the production of caramel, 97.
Ramaiah, N. A. and Vishnu	A new spectrophotometric method for the determination of copper with sodium versenate, 113.
Ramakrishnan, Alladi, Srinivasan, S. K., Ranganathan, N. R. and Vasudevan, R.	Multiple processes in electron-photon cascades, 311.
Ramakrishnan, Alladi and Srinivasan, S. K.	A note on cascade theory with ionisation loss, 133.
Raman, C. V. ..	The specific heats of some metallic elements, I, II, III, IV, 1, 7, 59, 139.
	The specific heats of crystals and the fallacy of the theories of Debye and Born, 273.
Ramanna, R. ..	*See* Deniz and others.
	See Iyengar and others.
Ramanna, R. and Navalkar, M. P.	On the determination of the slowing down length in ordinary water using a pulsed neutron source, 74.
Raman, P. S. ..	Oxidations with silver iodide dibenzoate, II, 65
	Heterocyclic compounds, IX, 260.
Ramavataram, K. ..	Raman effect studies in chelation, 47.
Ranganathan, N. R. ..	*See* Srinivasan and Ranganathan. *See* Ramakrishnan and others.
Rao, A. M. Jaya ..	*See* Puranik and Rao.
Rao, N. V. Subba and Ratnam, C. V.	Studies in the formation of heterocyclic rings containing nitrogen, III, 253.
Rao, P. S. and Sharma, R. K.	Studies on Indian plant gums: Composition and graded hydrolysis of gum Karaya (*Sterculia urens* Roxb.), 24.

Rao, S. K. Lakshmana		*See* Bhatnagar and Rao.
	..	Characteristic relations for the ultraspherical polynomials, 172.
	..	Addition of axially symmetric motions of viscous liquids, 418.
Ratnam, C. V.	..	*See* Rao and Ratnam.
Santhanam, M. S.	..	*See* Ramachandran and Santhanam.
Saraswat, H. C. and Agarwal, S. K. D.		Polarographic studies on the composition of nickel ferrocyanide complex, 91.
Sasisekharan, V. and Ramachandran, G. N.		Studies on collagen, II, 363.
Seshadri, T. R.	..	*See* Ahluwalia and others.
Seth, B. R.	..	New solutions for finite deformation, 105.
Shankar, Jagdish, Khubchandani, P. G. and Padmanabhan, V. M.		The crystal structure of magnesium acetate-tetrahydrate $Mg(CH_3COO)_2.4H_2O$, 117.
Sharma, R. K.	..	*See* Rao and Sharma.
Singh, B. K. and Verma, S. M.		Studies on the dependence of optical activity on chemical constitution, XLVI, 298.
Srinivasan, S. K.	..	*See* Ramakrishnan and Srinivasan.
	..	*See* Ramakrishnan and others.
Srinivasan, S. K. and Ranganathan, N. R.		Numerical calculations on the new approach to the cascade theory, I, II, 69, 268.
Srivastava, S. P.	..	*See* Farooqui and others.
Subbarao, B. N.	..	*See* Joshi and others.
Subrahmanya, R. S.	..	Polarographic behaviour of metals in ethanolamines, III, IV, 184, 195.
Swetharanyam, S.	..	On sums involving the fractional parts of numbers, 385.
Thosar, B. V.	..	*See* Joshi and others.
Umakanth, N.	..	*See* Iyengar and others.
Vasudevan, R.	..	*See* Ramakrishnan and others.
Verma, P. D.	..	*See* Verma and Bhatnagar.
Verma, S. M.	..	*See* Singh and Verma.
Vishnu	..	*See* Ramaiah and Vishnu.

TITLE INDEX

Addition of axially symmetric motions of viscous liquids (Rao), 418.

Bhabha's equation, non-relativitic approximation of (Gupta), 336.

BS-representations, certain, and a characterization of complete Boolean algebras (Balachandran), 35.

Cascade theory, the new approach, numerical calculations on, I, II (Srinivasan and Ranganathan), 69, 268.

Cascade theory with ionisation loss (Ramakrishnan and Srinivasan), 133.

Characteristic roots of the product of matrices (Khan), 84.

Chromatographic studies on the kinetics of the production of caramel (Ramaiah and others), 97.

Collagen, studies, II (Sasisekharan and Ramachandran), 363.

Colorimetric determinations, improvements, III (Khanna and others), 89.

Copper, determination, with sodium versenate, a new spectrophotometric method for (Ramaiah and Vishnu), 113.

Cosmic radiation, primary, solar anisotropy of, an interpretation (Nerurkar), 341.

Dalbergin and methyl dalbergin, a new synthesis, and a synthesis of allo-dalbergin (Ahluwalia and others), 293.

Dalbergin, constitution, III (Ahluwalia and others), 15.

Elastin, structure (Ramachandran and Santhanam), 124.

Electron-photon cascades, multiple processes (Ramakrishnan and others), 311.

Ferrite-core memory, two dimensional (Farooqui and others), 240.

Finite deformation, new solutions for (Seth), 105.

Flows, superposable (Bhatnagar and Verma), 281.

Gums, Indian plant, studies: composition and graded hydrolysis of gum Karaya (*Sterculia urens* Roxb.) (Rao and Sharma), 24.

Heterocyclic compounds, IX (Raman), 260.

Heterocyclic rings containing nitrogen, studies in the formation, III (Rao and Ratnam), 253.

Input and output system of the T.I.F.R. computer (Basu and Bakhru), 231.

Interference, generalised theory, and its applications, III (Pancharatnam), 402.

Magnesium acetate-tetrahydrate $Mg(CH_3COO)_2.4H_2O$, the crystal structure (Shankar and others), 117.

Motion of non-Newtonian viscous liquids, problems—general considerations (Bhatnagar and Rao), 161.

Neutrons from diffusing media, velocity distribution, time of flight method of studying (Deniz and others), 205.

Neutrons in beryllium oxide, slowing down and diffusion (Iyengar and others), 215.

Neutrons in beryllium oxide, slowing down and diffusion constants of, temperature dependence of (Iyengar and others), 224.

Nickel nitrate hexahydrate, optical properties and unit cell parameters (Jayaraman), 263.

Nuclear emulsions, inhibition of shrinkage (Krishnamoorthy), 327.

Optical activity, dependence of, on chemical constitution, studies, XLVI (Singh and Verma), 298.

Polarographic behaviour of metals in ethanolamines, III, IV (Subrahmanya), 184, 195.

Polarographic studies on the composition of nickel ferrocyanide complex (Saraswat and Agarwal), 91.

Polynomials, ultraspherical, characteristic relations (Rao), 172.

Quartz, the optical rotatory dispersion (Chandrasekhar), 147.

Raman effect in mixtures of pyridine with phenol, methanol and water (N - - - H hydrogen bond formation) (Puranik and Rao), 51.

Raman effect studies in chelation (Ramavataram), 47.

Samarium-153, decay (Joshi and others), 390.

Silver iodide dibenzoate, oxidations with, II (Raman), 65.

Slowing down length in ordinary water, determination, using a pulsed neutron source (Ramanna and Navalkar), 74.

Sn^{113}, carrier-free separation, from indium (Bhatki and Radhakrishna), 30.

Solvents, non-aqueous, investigations, II (Muniyappan and Anjaneyulu), 412.

Specific heats of crystals and the fallacy of the theories of Debye and Born (Raman), 273.

Specific heats of some metallic elements, I, II, III, IV (Raman), 1, 7, 59, 139.

Summability, some applications of Banach functional methods to (Parameswaran), 377.

Sums involving the fractional parts of numbers (Swetharanyam), 385.

Uniqueness of maximum pressure for the cubic form-function in the general theory of composite charges (Kapur), 177.

U_3O_8, pure, preparation, from crude sodium diuranate by intermediate complex formation (Krishnaprasad and Dadape), 20.

NOTICE TO AUTHORS

Scientific papers intended for publication in the *Proceedings of the Indian Academy of Sciences* can be accepted only when they are communicated by a Fellow of the Academy whose duty shall be to satisfy himself that such communications are fit to be read at the Meeting of the Academy and published in its *Proceedings*.

Papers should not ordinarily exceed fifty pages of foolscap. MSS. should be either typewritten or written in legible hand on one side of the paper. All papers should be carefully revised by the authors and should be absolutely in final form for printing. Position for text-figures should be indicated. Each paper shall conclude with a critical summary not exceeding 350 words.

Drawings, diagrams or other illustrations should be made on larger scale (preferably) twice the size than the ones in which they are intended to appear. They should be done in Indian ink on bristol board with lettering in pencil. Scale of magnification of camera lucida tracings should be indicated by the side of drawings. In certain special cases arrangements will also be made for monochrome lithographic and other colour plates. Reduction of illustrations desired should be indicated in pencil. Appropriate legends should accompany all drawings. Names of authors are to be marked in pencil on the left-hand corner of drawing sheets. Photomicrographs should be securely mounted with colourless paste.

All tables, quotations and footnotes which will be set hereafter (beginning from Vol. I, No. 2) in types smaller than the text, should be typewritten on separate sheets and placed with the text in proper sequence. Footnotes should be numbered in Arabic numerals.

References to literature in the text should be given, whenever possible, in chronological order, only the names of authors and years of publication, in brackets, being given. They should be cited in full after the summary, the authors' names following in alphabetical order. Thus,

Name or Names of author; Name of Journal (abbreviation) with a single underline; Year of publication; Number of Volume with a double underline, and lastly page. The following would be a useful illustration:—

Bergmann and Stather . . . . . Z. Physiol. Chem., 1926, 152, 189.

Two copies of slip-proof and wherever possible, a page proof for final revision will be sent to authors. All corrections are best made on the slip-proof which should be transmitted to the Office of the Academy. All proof corrections involve heavy expenses which would be negligible if the papers are carefully revised by the authors before submission.

Fifty free reprints including plates and with cover will be supplied for each paper. Additional copies can be supplied at cost on previous intimation.

Blocks appearing in the *Proceedings* will be available for purchase by their respective authors. Orders for the same should be sent along with the corrected proofs and in any case not later than one month after the date of publication of the paper. The price charged would be 25% of the actual cost of the blocks *plus* freight and despatching charges. If the blocks are reproduced in other journals or publications, due acknowledgment should be made in them to the *Proceedings*.

The original drawings and plates of blocks appearing in the *Proceedings* will be returned to such of the authors as may require them provided the cost of despatching such originals is borne by them.

CONTENTS

PAGE

Studies on Collagen. II. Cylindrical Lattice Structure of Collagen . . . . . V. Sasisekharan and G. N. Ramachandran 363

Some Applications of Banach Functional Methods to Summability . . . . . M. R. Parameswaran 377

On Sums Involving the Fractional Parts of Numbers . . S. Swetharanyam 385

Decay of Samarium-153 . . M. C. Joshi, B. N. Subbarao and B. V. Thosar 390

Generalised Theory of Interference and Its Applications. Part III. Interference Figures in Transparent Crystals . . . . S. Pancharatnam 402

Investigations in Non-Aqueous Solvents. Part II. Solubility and Conductances of Some Rare Earth Metal and Thorium Acetates in Ethylenediamine . . . . . T. Muniyappan and B. Anjaneyalu 412

Addition of Axially Symmetric Motions of Viscous Liquids . . . . . S. K. Lakshmana Rao 418

5992